SPIN POLARIZATION EFFECT ON IGNITION ACCESS CONDITION FOR D-T AND D-^{3}He TOKAMAK FUSION REACTORS

D-^{3}He/FUSION REACTORS

KEYWORDS: *spin polarization, ignition criterion, D-T and D-^{3}He tokamak reactors*

OSAMU MITARAI *Kumamoto Institute of Technology*
Department of Electrical Engineering, Ikeda 4-22-1, Kumamoto 860 Japan

HIROKI HASUYAMA *Kurume Institute of Technology*
Department of Physics, 2228 Kamitsu-machi, Kurume, 830 Japan

YOSHIHISA WAKUTA *Kyushu University*
Department of Applied Nuclear Engineering
Hakozaki, Higashi-ku, Fukuoka, 812 Japan

Received February 11, 1991
Accepted for Publication June 11, 1991

Ignition characteristics in deuterium-tritium (D-T) and D-^{3}He tokamak reactors with spin-polarized fuels are presented by using the ignition access condition based on the generalized saddle point in the representation of ($\bar{P}_{ht}\tau_E^2$, $n\tau_E$, T). Enhancement of the D-T fusion cross section due to parallel spin polarization with respect to the magnetic field can reduce the confinement enhancement factor required for reaching ignition by ~20% if fusion particle loss is not induced by the anisotropic fusion particle distribution. Spin polarization is thus effective when a D-T reactor is marginal for ignition. In D-^{3}He fusion, it is more advantageous to use spin-polarized fuel in the heating phase than in the case of D-T fusion. The ignition toroidal beta value can be reduced by spin polarization from 12 ± 0.8 to 5.3 ± 0.5% in D-^{3}He = 2:1 plasma and from 17 ± 0.5 to 6.5 ± 0.2% in D-^{3}He = 1:1 plasma. The auxiliary heating power to reach ignition, which is rather large for D-^{3}He fusion, can be reduced by a factor of 2 to 3 compared with the unpolarized case. For example, in the D-^{3}He Tokamak Reactor, 350 MW of auxiliary heating power for D:^{3}He = 2:1 and $T_i(0)/T_e(0) = 1$ without spin polarization can be reduced to 190 MW with complete polarization of the deuterium and ^{3}He ions. The deuterium-deuterium fusion suppression effect, if it exists, does not alter the ignition condition much. Various problems related to the spin polarization scheme are also discussed.

I. INTRODUCTION

In recent design studies of deuterium-tritium (D-T) fusion reactors, the confinement enhancement factor required for reaching ignition has been a major concern.[1-4] As it is difficult to achieve a large confinement enhancement factor to reach ignition, it is desirable to try to reduce it somehow. The selection of higher plasma currents is one choice that can be made in a design to try to reduce the confinement enhancement factor. Parallel spin of polarization of deuterium and tritium ions with respect to the magnetic field can enhance the fusion cross section by 50% (Ref. 5); therefore, the confinement enhancement factor can be reduced because the ignition regime becomes wider.

The recent discovery of ^{3}He resources on the lunar surface[6] has stimulated efforts to design a neutron-lean D-^{3}He reactor.[7-10] The plasma current, toroidal magnetic field, auxiliary heating power, and toroidal beta value must be larger than those in a D-T tokamak reactor to reach ignition in a D-^{3}He tokamak reactor as long as the present confinement scaling law is applied.[7] If fusion nuclei such as deuterium and ^{3}He ions are 100% vector polarized parallel to the magnetic field, the fusion cross section is increased by almost 50% (Ref. 5), which can ease the fusion conditions and

reduce the auxiliary heating power required for reaching ignition. This condition, however, is very difficult to achieve during the formation of polarized nuclei or pellets. In our analysis, depolarization of the fusing nuclei in the fusion reactor has been neglected. On the other hand, depolarization, which takes place during the formation of the polarized nuclei or pellets and is induced by magnetic fluctuations and by recycling on the first wall, cannot be avoided completely. Therefore, a 50% increment in the fusion cross section can be achieved in the ideal case. If deuterium-deuterium (D-D) reactions are suppressed by parallel spin polarization, which is, however, still controversial,[11-14] an aneutronic "clean" fusion reactor could be constructed. Thus, the spin polarization effect is much more attractive in a D-^{3}He fusion reactor than in a D-T reactor.

The plasma operating parameter contour (POPCON) analysis in the (n, T) plane has been used to discuss the ignition condition in a tokamak reactor.[15,16] This method can only be applied to see the ignition capability in a specific device. On the other hand, we have proposed a complementary method to discuss the ignition capability of a reactor: the saddle point condition, $(\gamma_H C_{op})^2 > [\bar{P}_{ht}\tau_E^2]_{SDL}$, holding for the power law scaling $\tau_E = \gamma_H C_{op}/\bar{P}_{ht}^{0.5}$ (Refs. 17 and 18). Here $\bar{P}_{ht}$ is the sum of the ohmic heating and auxiliary heating power density; $[\bar{P}_{ht}\tau_E^2]_{SDL}$ is the height of the generalized saddle point in the generalized ignition contour map $(\bar{P}_{ht}\tau_E^2, n\tau_E, T)$; C_{op} is the coefficient in the scaling; and γ_H is the confinement enhancement factor. The product of the auxiliary heating power density and the square of the energy confinement time is constant as $[\bar{P}_{ht}\tau_E^2] = (\gamma_H C_{op})^2$ during tokamak operation, if confinement is not affected by alpha-particle heating and radiative power loss, and L-mode confinement scaling of the form $\tau_E \propto \bar{P}_{ht}^{-0.5}$ applies. This means that the contour lines of $[\bar{P}_{ht}\tau_E^2]$, obtained from the global power balance equation, on the $n\tau_E$-T plane corresponds to the constant height of the operation path. Thus, a tokamak reactor with a higher operation path $(\gamma_H C_{op})^2$ than the saddle point $[\bar{P}_{ht}\tau_E^2]_{SDL}$ in the contour map can reach ignition. In this method, as opposed to the POPCON analysis, the height of the saddle point is easily obtained from a quadratic form, and its value can be used for determining the reactor parameters and confinement enhancement factor for any tokamak.

Even if the confinement is degraded by alpha-particle heating, the saddle point method is still useful. Especially when confinement is degraded by net heating power, including alpha-particle heating $\bar{P}_\alpha$ and bremsstrahlung loss $\bar{P}_b$ effect, as $\tau_E = \gamma_H C_{op}/(\bar{P}_{ht} + \bar{P}_\alpha - \bar{P}_b)^{0.5}$, the ignition capability in D-T fusion can be discussed as in the case without $\bar{P}_\alpha$ and $\bar{P}_b$, and ignition is accessible when $(\gamma_H C_{op})^2 \geq 4[\bar{P}_{ht}\tau_E^2]_{SDL}$ is satisfied (ignition access condition).[19] A factor of 4 is added to the former criterion, which comes from the quadratic form of the global power balance equation, together with the net heating power. While the confinement time becomes almost infinite in the ignition regime $(\bar{P}_{ht} = 0)$ for $\tau_E = \gamma_H C_{op}/\bar{P}_{ht}^{0.5}$, the confinement time given by $\tau_E = \gamma_H C_{op}/(\bar{P}_{ht} + \bar{P}_\alpha - \bar{P}_b)^{0.5}$ is finite in the ignition regime and changes with n and T. The ignition access condition does not depend on the heating process, and one can quickly decide whether a tokamak reactor can reach ignition or not for various plasma parameters with the use of the height of the saddle points. Thus, we can easily determine the confinement enhancement factor required for reaching ignition and know the overall ignition capability of various tokamak reactors.

Reaching D-^{3}He ignition can be discussed by the same method by replacing $\bar{P}_\alpha$ by $\bar{P}_F$, where $\bar{P}_F$ is the total fusion power from D-D and D-^{3}He fusion, and $\bar{P}_b$ by $(\bar{P}_b + \bar{P}_s)$, where $\bar{P}_s$ is the synchrotron radiation loss dominant in D-^{3}He fusion. We apply this ignition access condition to consider the effect of spin polarization on the ignition capability of D-T and D-^{3}He fusion reactors. Preliminary results for a D-^{3}He tokamak fusion reactor were presented in Ref. 20.

The fusion cross section is increased at most by 50% for both D-T and D-^{3}He fuel ions by complete spin polarization. However, its effect on the ignition condition is larger in a D-^{3}He reactor. As seen in the following D-T and D-^{3}He fusion reactions,

$$\mathrm{D} + \mathrm{T} \rightarrow {}^4\mathrm{He}\ (3.52\ \mathrm{MeV}) + {}^1n\ (14.0\ \mathrm{MeV})$$

and

$$\mathrm{D} + {}^3\mathrm{He} \rightarrow p\ (14.7\ \mathrm{MeV}) + {}^4\mathrm{He}\ (3.7\ \mathrm{MeV})\ ,$$

only charged particles can affect the ignition condition. Since alpha-particle heating power increases equivalently by 3.52 MeV × 0.5 = 1.76 MeV in D-T fusion and neutron power increases also equivalently by 14.0 × 0.5 = 7 MeV in the blanket, only the 1.76-MeV alpha-particle heating power is available to relax the ignition condition. On the other hand, heating power from charged particles such as protons and alpha particles in D-^{3}He fusion increases equivalently by (14.7 × 0.9 + 3.7) MeV × 0.5 = 8.465 MeV with the use of $\eta_{p14} = 0.9$ given in Sec. II. Thus, we expect that the spin polarization effect is larger in a D-^{3}He reactor than in a D-T reactor.

In this paper, we evaluate the spin polarization effect on the height of the generalized saddle point and obtain the confinement enhancement factor required for reaching ignition in a D-T tokamak reactor with the ignition access condition. The auxiliary heating power is also estimated for D-T spin-polarized fusion. In a D-^{3}He tokamak reactor, we demonstrate that the beta value together with the confinement enhancement factor required for reaching ignition can immediately be determined by the ignition access condition. We also further estimate the auxiliary heating power required

to reach the ignition regime using the POPCON method for both unpolarization and spin polarization. We also demonstrate that D-D fusion suppression has little effect on the ignition condition. Throughout this paper, parallel spin polarization is assumed to be maintained without appreciable depolarization for a sufficient time for reactions to occur.

This paper is organized as follows: In Sec. II, the ignition access condition for D-T and D-^{3}He fusion is derived based on the generalized saddle point; the height of the operation path and the generalized saddle point are given. In Secs. III and IV, calculated results of spin polarization effects in D-T and D-^{3}He fusion reactors are presented, respectively. In Secs. V and VI, a discussion and summary are given.

II. IGNITION ACCESS CONDITION FOR D-T AND D-^{3}He FUSION REACTORS

The possibility of reaching ignition in both D-T and D-^{3}He tokamak reactors with a power law scaling such as the Goldston type, with net heating power, can be discussed by the ignition access condition proposed previously.[19] This condition is derived from the concept of the "operation path" of a reactor and the ignition boundary on the $(n\tau_E, T)$ plane and is finally based on the generalized saddle point.

II.A. Ignition Access Condition and the Height of the Generalized Saddle Point

We summarize briefly how the ignition access condition in a D-T and a D-^{3}He fusion reactor can be derived. The operation path of a reactor can be obtained by the combination of the confinement scaling law,

$$\tau_E = \frac{\gamma_H C_{op}}{(\bar{P}_{ht} + \bar{P}_F - \dot{W} - \bar{P}_b - \bar{P}_s)^{0.5}} , \tag{1}$$

and the global power balance equation,

$$\dot{W} = (\bar{P}_{ht} + \bar{P}_F - \bar{P}_b - \bar{P}_s) - \bar{P}_L , \tag{2}$$

where

$\dot{W}$ = time derivative of the plasma energy

$\bar{P}_L$ = plasma conduction loss

$\bar{P}_{ht}$ = sum of the auxiliary and ohmic heating powers

$\bar{P}_F$ = fusion power, composed of the D-T fusion in a D-T reactor and the D-^{3}He and D-D fusion in a D-^{3}He reactor

$\bar{P}_b$ = bremsstrahlung loss

$\bar{P}_s$ = synchrotron radiation loss.

An overbar indicates a volume-averaged quantity over the density and temperature profiles $[n_e(x) = n_e(0) \times (1 - x^2)^{\alpha_n}$ and $T_i(x)/T_i(0) = T_e(x)/T_e(0) = (1 - x^2)^{\alpha_T}]$. Thus, $\bar{P}_L = A_L n_e(0)/\tau_E$, $\bar{P}_F = A_F n_e(0)^2$, $\bar{P}_b = A_b n_e(0)^2$, and $\bar{P}_s = A_s n_e(0)^2$ are given, where coefficients A_L to A_s are described in the Appendix for D-T and D-^{3}He fusion reactors.

Inserting Eq. (2) into Eq. (1) provides the operation path:

$$[n_e(0)\tau_E]_{op} = \frac{(\gamma_H C_{op})^2}{A_L} . \tag{3}$$

On the other hand, the ignition boundary is given by Eq. (2) with $\bar{P}_{ht} = 0$ and $\dot{W} = 0$ as

$$[n_e(0)\tau_E]_{ig} = \frac{A_L}{(A_F - A_b - A_s)} . \tag{4}$$

Ignition is accessible when $[n_e(0)\tau_E]_{op} > [n_e(0)\tau_E]_{ig}$ is satisfied; then, the following relationship is obtained:

$$\begin{aligned}(\gamma_H C_{op})^2 &\geq 4\left[\frac{A_L^2}{4(A_F - A_b - A_s)}\right] \\ &\geq 4 \min\left[\frac{A_L^2}{4(A_F - A_b - A_s)}\right] , \\ &= 4[\bar{P}_{ht}\tau_E^2]_{\mathrm{SDL}} ,\end{aligned} \tag{5}$$

where $[\bar{P}_{ht}\tau_E^2]_{\mathrm{SDL}}$ is given by the minimum value of the maximum of $[\bar{P}_{ht}\tau_E^2]$, which is obtained by multiplying τ_E^2 on both sides of Eq. (2) in the steady state $(\dot{W} = 0)$ as

$$\begin{aligned}[\bar{P}_{ht}\tau_E^2] &= -(A_F - A_b - A_s) \\ &\quad \times \left[n(0)\tau_E - \frac{A_L}{2(A_F - A_b - A_s)}\right]^2 \\ &\quad + \frac{A_L^2}{4(A_F - A_b - A_s)} ,\end{aligned} \tag{6}$$

and hence,

$$[\bar{P}_{ht}\tau_E^2]_{\mathrm{SDL}} = \min\left[\frac{A_L^2}{4(A_F - A_b - A_s)}\right] , \tag{7}$$

which is called the height of the "generalized" or "normalized" saddle point. We calculate this important quantity for given parameters in D-T and D-^{3}He fusion reactors.

For D-T fusion, we use parameters describing the parabolic profiles of the temperature and density $(\alpha_n = \alpha_T = 1)$, the alpha particle-heating efficiency $(\eta_\alpha = 1)$, an average electric charge number for impurities $(Z = 7)$, the effective ion charge $(Z_{eff} = 1.5)$, and the fraction of alpha particle to electron density $(f_\alpha = n_\alpha/n_e = 0.05)$, and we assume an isothermal plasma with $T_i(0) = T_e(0) = T(0)$ in this calculation for simplicity.

For impurity-free $(f_{imp} = n_{imp}/n_e = 0)$ D-^{3}He plasmas without accumulation of D-^{3}He fusion products $(f_\alpha = 0$ and $f_{p14} = n_{p14}/n_e = 0)$, we obtain $f_{\mathrm{D}} = n_{\mathrm{D}}/n_e = \frac{1}{3}$, $f_{^3\mathrm{He}} = n_{^3\mathrm{He}}/n_e = \frac{1}{3}$, and $Z_{eff} = \frac{5}{3}$ for a

D:^{3}He = 1:1 fuel mixture and $f_D = \frac{1}{2}$, $f_{^3He} = \frac{1}{4}$, and $Z_{eff} = 1.5$ for a D:^{3}He = 2:1 fuel mixture using the charge neutrality condition. Other parameters are chosen such that the heating efficiencies of alpha particles in D-^{3}He fusion and D-D fusion products are $\eta_\alpha = \eta_{p3} = \eta_T = \eta_{^3He} = 1$, the heating efficiency of a 14.7-MeV proton is $\eta_{p14} = 0.9$, the hole fraction is $f_H = 0.1$, and the effective reflection coefficient from the first wall is assumed to be $R_{eff} = 0.965$. Although hot-ion mode operation is favorable[7] and should be realized during the heating phase in a D-^{3}He reactor, we chose equal ion and electron temperatures [$T_i(0) = T_e(0) = T(0)$] throughout this paper to see the spin polarization effect. (Some results on hot-ion mode operation are also presented.)

II.B. Height of the Operation Path for D-T and D-^{3}He Tokamak Reactors

The height of the operation path, which is provided by the confinement scaling law, is an indicator of the ignition capability. A reactor with a higher operation path can reach ignition more easily. In this study, we use two scaling laws: the Goldston scaling law,[21]

$$\tau_E(\text{Goldston})\ (\text{s}) = \gamma_H\, 6.4\times10^{-8}(A_i/1.5)^{0.5} I_p\ (\text{A})\, R^{1.75}\ (\text{cm}) \times a^{-0.37}\ (\text{cm})\, \kappa^{0.5}/\sqrt{P_{HT}}\ (\text{W}) = \gamma_H C_{op}(G)/\sqrt{\bar{P}_{ht}}\ (\text{MW/m}^3)\ , \quad (8)$$

and the ITER89 power scaling law,[22]

$$\tau_E(\text{ITER89P})\ (\text{s}) = \gamma_H\, 0.048 A_i^{0.5} I_p^{0.85}\ (\text{MA})\, R^{1.2}\ (\text{m})\, a^{0.3}\ (\text{m})\, \kappa^{0.5} \times B_t^{0.2}\ (\text{T})\, \bar{n}^{0.1}\ (\times 10^{20}\ \text{m}^{-3})/\sqrt{P_{HT}}\ (\text{MW}) = \gamma_H C_{op}(\text{ITER89P})/\sqrt{\bar{P}_{ht}}\ (\text{MW/m}^3)\ , \quad (9)$$

where

γ_H = confinement enhancement factor ($\gamma_H = 1$ corresponds to the L mode)

A_i = mass correction factor (2.5 for D-T and D-^{3}He plasmas)

and the total heating power P_{HT} is replaced by $\bar{P}_{ht} \times 2\pi^2 R a^2 \kappa$. From Eqs. (8) and (9), we obtain the height of the operation path as follows:

$$(\gamma_H C_{op})^2(\text{Goldston})\ (\text{MW/m}^3\cdot\text{s}^2) = [\bar{P}_{ht}\tau_E^2]_{op} = \gamma_H^2\, 2\times10^{-16}(A_i/1.5) I_p^2\ (\text{A}) \times (R/a)^{2.5} a^{-0.24}\ (\text{cm}) \quad (10)$$

and

$$(\gamma_H C_{op})^2(\text{ITER89P})\ (\text{MW/m}^3\cdot\text{s}^2) = [\bar{P}_{ht}\tau_E^2]_{op} = \gamma_H^2 1.167\times10^{-4} A_i I_p^{1.7}\ (\text{MA}) \times (R/a)^{1.4} B_t^{0.4}\ (\text{T})\, \bar{n}^{0.2}\ (\times 10^{20}\ \text{m}^{-3})\ , \quad (11)$$

respectively. Note that the triangularity factor in estimating the plasma volume in P_{HT} has been neglected. Calculated values of the height of the operation path C_{op}^2 for $\gamma_H = 1$ are listed in Table I for the planned next-generation tokamaks[1-4] and proposed D-^{3}He tokamak reactors, such as the Alternating Current Tokamak Reactor Upgrade[7] (ACTR-U), where the plasma current is reversed alternatively after ohmic heating current is saturated,[23] the D-^{3}He Tokamak Reactor (DHETR) with a crescent plasma shape operable in the high-beta first stability regime,[7] and the Apollo tokamak reactor recently proposed.[8] In the calculation of C_{op}^2(ITER89P), the values of the average line electron density $\bar{n}$ are taken to be 1×10^{20} m^{-3} and 5×10^{20} m^{-3} for the D-T and D-^{3}He tokamak reactors as a reference, respectively. As seen in Table I,

TABLE I

Height of the Operation Path for D-T and D-^{3}He Tokamak Reactors

Reactor	R (m)	a (m)	B_t (T)	q_a	κ	δ	I_p (MA)	$\langle\beta\rangle_{TROY}$ (%)[a]	C_{op}^2 (MW/m$^3\cdot$s^2) Goldston	C_{op}^2 (MW/m$^3\cdot$s^2) ITER89P[b]
CIT (Ref. 1)	2.14	0.66	11.0	2.5	2.0	0.249	12.3	5.9	0.362	0.282
NET (Ref. 2)	6.3	2.0	6.0	2.557	2.2	0.3	25.0	7.3	1.067	0.708
FER (Ref. 3)	4.7	1.6	5.2	2.965	2.0	0.4	15.0	6.3	0.340	0.255
ITER-P (Ref. 4)	5.8	2.2	5.0	2.5	1.9	0.303	22.0	7.0	0.518	0.413
ACTR-U (Ref. 7)	10	2	10	2.5	2.0	0.306	23.0	4.0	2.87	1.99
	10	2.645	10	2.5	2.0	0.3	40.0	5.3	4.04	3.49
DHETR (Ref. 7)	6	2	10	2.5	2.1	1[c]	79.4[c]	13.9	9.52	7.99
Apollo (Ref. 8)	6.1	2.42	9.19	2.04	2.2	0.4	80.0	12.6	5.98	6.13
	8	2.01	12.9	2.32	2.2	0.3	47.1	6.3	6.78	5.41

[a]The Troyon beta limit is given by $\langle\beta\rangle_{TROY}(\%) = 3.5 I_p/(aB_t)$.
[b]C_{op}^2 (ITER89P) is obtained at $\bar{n} = 1\times10^{20}$ m^{-3} for D-T tokamaks and at $\bar{n} = 5\times10^{20}$ m^{-3} for D-^{3}He tokamaks.
[c]Crescent-shaped plasma.

C_{op}^2 (Goldston) is larger than C_{op}^2 (ITER89P); in other words, the Goldston scaling is more favorable than the ITER89 power law scaling in most cases.

III. SPIN POLARIZATION EFFECT IN A D-T FUSION REACTOR

An enhancement of the fusion cross section due to parallel spin polarization can increase the fusion alpha-particle heating and hence relax the fusion condition unless alpha-particle loss is induced by an anisotropic alpha-particle birth distribution.[24] We present calculated results with and without the spin polarization effect on the ignition access condition for comparison with the assumption of no alpha-particle loss.

III.A. D-T Spin Polarization Effect on the Generalized Ignition Contour Map

Generalized ignition contour maps and operation paths for next-generation D-T tokamak reactors are shown in Fig. 1a with unpolarization [γ_{spin}(D-T) = 1] and in Fig. 1b with complete spin polarization [γ_{spin}(D-T) = 1.5]. Operation paths based on the Goldston scaling law for the Compact Ignition Tokamak (CIT), International Thermonuclear Experimental Reactor-Physics Phase (ITER-P), and Next European Tokamak (NET) are indicated by the dotted, dash-dotted, and dashed lines, respectively, for $\gamma_H = 1$ (L mode) and $\gamma_H = 1.5$ (improved L mode). The operation path for CIT with $\gamma_H = 1.5$ does not enter into the ignition regime for the unpolarized case, as shown in Fig. 1a. On the other hand, with complete spin polarization, as in Fig. 1b, the operation path goes through the ignition regime. Note that the operation path itself is exactly the same for the cases with and without spin polarization; only the contour map changes.

Although reaching ignition is impossible in the unpolarized case, even with the use of an infinitely large auxiliary heating power, a finite heating power can make ignition possible for complete spin polarization. Spin polarization can thus make a big difference in the heating power when the ignition is marginal, as has also been pointed out by Furth.[25]

For ITER-P and NET, ignition is accessible in both the γ_{spin}(D-T) = 1 and 1.5 cases. The ignition regime of ITER-P determined by the intersection between the operation path and the ignition boundary is narrow along the temperature axis, as seen in Fig. 1a for the unpolarization case. When we calculate the minimum heating power at the Cordey pass in the POPCON analysis for the same parameters,[19] we obtain the total heating power including the ohmic heating power as P_{HT}(ITER-P) = 0.0205 (MW/m^3) × 1052.8 (m^3) = 21.58 (MW) and P_{HT}(NET) = 0.0152 (MW/m^3) × 1094.3 (m^3) = 16.63 (MW) for the unpolarization case, and P_{HT}(ITER-P) = 0.0156 (MW/m^3) × 1052.8 (m^3) = 16.42 (MW) and P_{HT}(NET) = 0.0126 (MW/m^3) × 1094.3 (m^3) = 13.78 (MW) for the case with complete spin polarization. Thus, we see that 5.16 and 2.85 MW of auxiliary heating power can be saved by complete spin polarization in the ITER-P and NET tokamaks, respectively. Note that the total heating power calculated here is the minimum heating power for surmounting the Cordey pass; hence, it takes an infinitely long time to reach ignition at this heating power. A somewhat larger heating power is necessary to reach ignition within a certain time in actual operation. Thus, ~15 and 9 MW of heating power can be

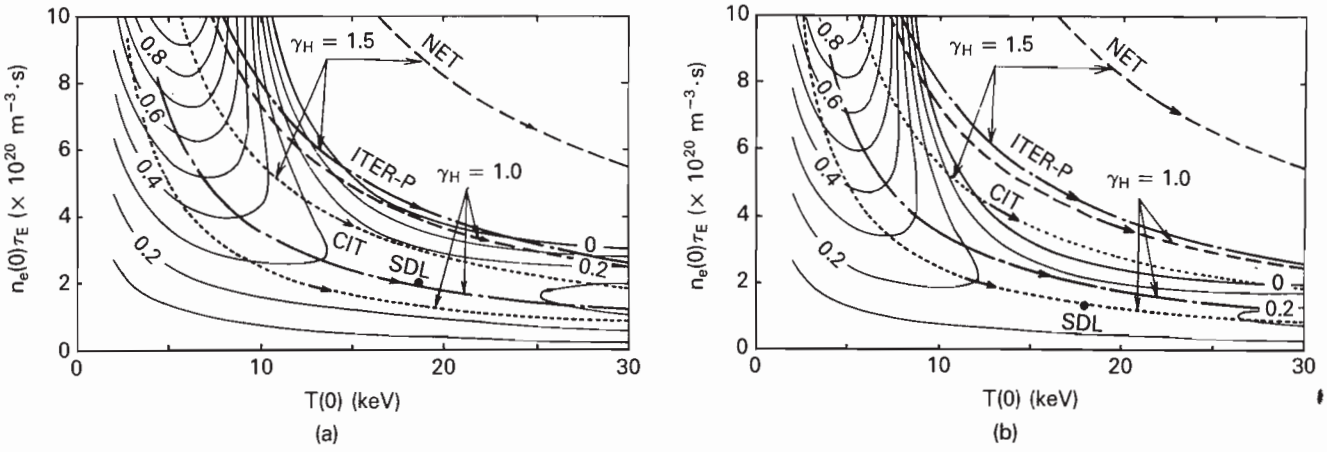

Fig. 1. Operation paths calculated with Goldston scaling for the CIT, NET, and ITER-P D-T tokamak reactors on the generalized ignition contour map ($\bar{P}_{ht}\tau_E^2, n\tau_E, T$) in the case of (a) no spin polarization [γ_{spin}(D-T) = 1] and (b) complete spin polarization [γ_{spin}(D-T) = 1.5]. Other plasma parameters are $\alpha_T = \alpha_n = 1$, $Z_{eff} = 1.5$, $f_\alpha = 0.05$, $Z = 7$, $\eta_\alpha = 1$, and $T_i(0) = T_e(0) = T(0)$. Spacing of the contour lines is in units of megawatts per cubic metre per second squared. The saddle point is denoted by "SDL" and the ignition boundary by "0."

saved if three times the foregoing values is employed, respectively.

The dependence of the height of the generalized saddle point on the degree of spin polarization γ_{spin}(D-T) is shown in Fig. 2 for various profile parameters $\alpha_n = \alpha_T$ in the ideal case of $Z_{eff} = 1$, $f_\alpha = 0$, $\eta_\alpha = 1$, and $T_i(0)/T_e(0) = 1$. With complete spin polarization, the height of the generalized saddle point becomes ~30% lower. If depolarization takes place, the degree of spin polarization has an intermediate value between 1 and 1.5 given by γ_{spin}(D-T) = 1 + $0.5\boldsymbol{P}_{ZD}\cdot\boldsymbol{P}_{ZT}$, where $\boldsymbol{P}_{ZD}$ is the vector polarization of deuterons and $\boldsymbol{P}_{ZT}$ is the vector polarization of tritons.[26] The height of the generalized saddle point can be obtained from Fig. 2 at the corresponding value of γ_{spin}(D-T).

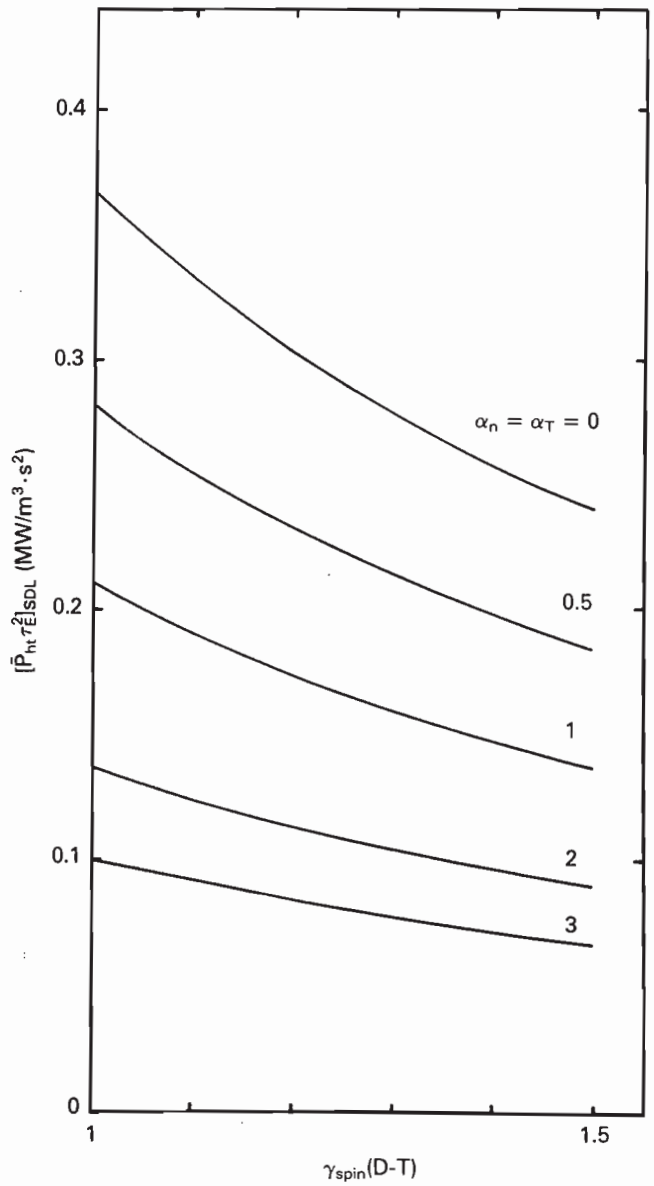

Fig. 2. Height of the generalized saddle point versus spin polarization factor γ_{spin}(D-T) for various profile parameters $\alpha_T = \alpha_n$.

III.B. Confinement Enhancement Factor for Reaching D-T Ignition

The confinement enhancement factor required for reaching ignition can be obtained from the $(\gamma_H C_{op})^2$ versus γ_H curves presented earlier.[19] Figure 3a shows $(\gamma_H C_{op})^2$ curves together with the lateral lines of $4[\bar{P}_{ht}\tau_E^2]_{SDL}$ for γ_{spin}(D-T) = 1 and 1.5 for CIT. Plasma parameters are $\alpha_n = \alpha_T = 1$, $Z_{eff} = 1.5$, $f_\alpha = 0.05$, $Z = 7$, $\eta_\alpha = 1$, and $T_i(0)/T_e(0) = 1$. The average line electron density $\bar{n}$ ($= \bar{n}_{20} \times 10^{20}$ m^{-3}) is varied from 0.8 to 7×10^{20} m^{-3} for the ITER89 power law scaling. Since the height of the generalized saddle point becomes lower because of spin polarization, the confinement enhancement factor required for reaching ignition is also reduced, as shown in Fig. 3. Critical confinement enhancement factors are, for example, 1.74 for the Goldston scaling and 1.97 to 1.65 for $\bar{n} = 2$ to 7×10^{20} m^{-3} with the ITER89 power law in the case of unpolarization, where $[\bar{P}_{ht}\tau_E^2]_{SDL} = 0.2745$ MW/m^3·s^2. For the case of complete spin polarization, where $[\bar{P}_{ht}\tau_E^2]_{SDL} = 0.175$ MW/m^3·s^2, the critical values of γ_H are 1.39 for Goldston scaling and 1.58 to 1.32 for $\bar{n} = 2$ to 7×10^{20} m^{-3} with the ITER89 power law. Note that since the ohmic heating power is not subtracted in the ignition access condition, the actual value of γ_H may be slightly smaller. Thus, we can easily find the approximate value of the confinement enhancement factor required for reaching ignition.

The $(\gamma_H C_{op})^2$ curves for NET, the Fusion Engineering Reactor (FER), and ITER-P are shown in Figs. 3b, 3c, and 3d, respectively. Note that NET can enter the ignition regime in the L-mode scaling law with complete spin polarization. In Fig. 3d, the $(\gamma_H C_{op})^2$ curve for the ITER89 power law with $\bar{n} = 3 \times 10^{20}$ m^{-3} is similar to the curve for the Goldston scaling. Thus, the critical confinement enhancement factor can easily be obtained from these figures.

Critical values of γ_H thus obtained are listed in Table II. We have found that the critical values of γ_H can be reduced by almost 20% with D-T spin polarization.

IV. SPIN POLARIZATION EFFECT IN A D-^{3}He FUSION REACTOR

In the neutron-lean D-^{3}He tokamak reactor, the ignition access condition can be used in the same way as in a D-T reactor. The operation paths for the most optimistic scaling ($\tau_E = \gamma_H C_{op}/\bar{P}_{ht}^{0.5}$), the most pessimistic scaling with confinement degradation due to the heating power of 14.7-MeV protons [$\tau_E = \gamma_H C_{op}/$

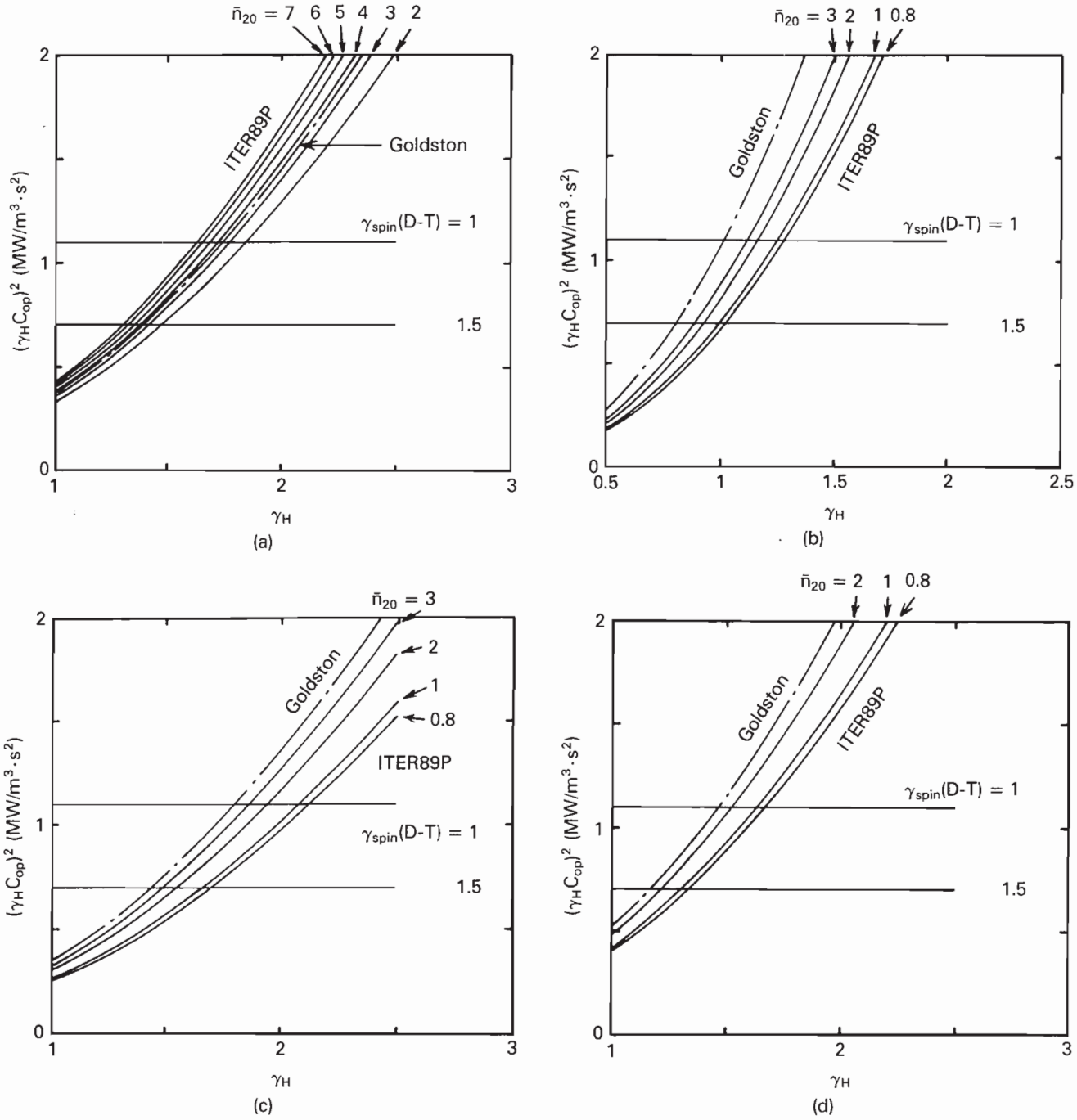

Fig. 3. Height of the operation path for Goldston $[\gamma_H C_{op}(G)]^2$ and ITER89P $[\gamma_H C_{op}(\mathrm{IT89P})]^2$ scaling versus the confinement enhancement factor γ_H with $\bar{n}_{20}$ ($\times 10^{20}$ m^{-3}) as a parameter for (a) CIT, (b) NET, (c) FER, and (d) ITER-P. The machine parameters are listed in Table I.

$(\bar{P}_{ht} + \bar{P}_{p14})^{0.5}$], and an intermediate case between the scaling laws employed in this paper [$\tau_E = \gamma_H C_{op}/(\bar{P}_{ht} + \bar{P}_F - \bar{P}_b - \bar{P}_s)^{0.5}$], are shown in Fig. 4. Since the first two cases are discussed in detail in Ref. 7, we consider the third type of operation path including the case of a D-T fusion reactor.[19] Note that $\dot{W}$ in Eq. (1) is taken to be zero in the following section.

IV.A. D-^{3}He Spin Polarization Effect on the Generalized Ignition Contour Map

Figure 4a shows the generalized ignition contour map and operation paths for a toroidal beta value of $\langle\beta\rangle = 10\%$ and unpolarization. Other plasma parameters are $\alpha_n = \alpha_T = 1$, $f_D = f_{^3He} = \frac{1}{3}$, $Z_{eff} = \frac{5}{3}$,

TABLE II

Confinement Enhancement Factors in D-T Tokamak Reactors for Unpolarization and Spin Polarization*

Reactor	γ_{spin} (D-T)	Goldston γ_H	ITER89 Power Law, γ_H [$\bar{n}$ ($\times 10^{20}$ m^{-3})]							
			0.8	1.0	2.0	3.0	4.0	5.0	6.0	7.0
CIT	1	1.74			1.97	1.84	1.77	1.72	1.68	1.55
	1.5	1.39			1.58	1.47	1.41	1.37	1.34	1.32
NET	1	1.01	1.27	1.24	1.16	1.12				
	1.5	0.81	1.01	0.99	0.93	0.89				
FER	1	1.8	2.12	2.08	1.93	1.86				
	1.5	1.43	1.70	1.66	1.55	1.49				
ITER-P	1	1.45	1.67	1.63	1.52	1.45				
	1.5	1.16	1.33	1.30	1.21	1.16				

*Parameters are $\alpha_n = \alpha_T = 1$, $Z_{eff} = 1.5$, $f_\alpha = 0.05$, $Z = 7$, $\eta_\alpha = 1$, and $T_i(0)/T_e(0) = 1$.

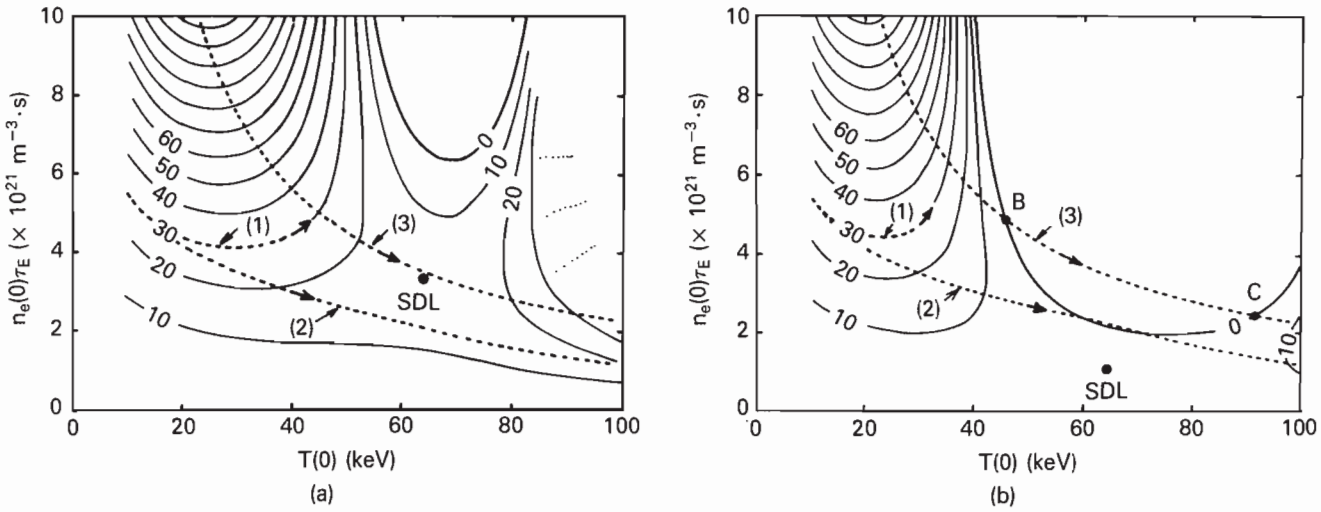

Fig. 4. Operation paths with $(\gamma_H C_{op})^2 = 30$ MW/m$^3\cdot$s^2 for ACTR-U on the generalized ignition contour map $(\bar{P}_{ht}\tau_E^2, n\tau_E, T)$ in the case of (a) no spin polarization [γ_{spin}(D-^{3}He) = 1] and (b) complete spin polarization [γ_{spin}(D-^{3}He) = 1.5] for $\langle\beta\rangle = 10\%$. Other plasma parameters are $\alpha_T = \alpha_n = 1$, $f_D = f_{^3He} = \frac{1}{3}$, $Z_{eff} = \frac{5}{3}$, $f_p = f_\alpha = 0$, $R_{eff} = 0.965$, $T_i(0) = T_e(0) = T(0)$, and γ_{spin}(D-D) = 1. Spacing of the contour lines is in units of MW/m$^3\cdot$s^2. Dotted lines (1), (2), and (3) indicate the operation paths with $\tau_E = \gamma_H C_{op}/\bar{P}_{ht}^{0.5}$, $\tau_E = \gamma_H C_{op}/(\bar{P}_{ht} + \bar{P}_{p14})^{0.5}$, and $\tau_E = \gamma_H C_{op}/(\bar{P}_{ht} + \bar{P}_F - \bar{P}_b - \bar{P}_s)^{0.5}$, respectively.

$f_{p14} = f_\alpha = 0$, $R_{eff} = 0.965$, $T_i(0) = T_e(0) = T(0)$, and ACTR-U ($R = 10$ m and $a = 2$ m). None of the operation paths can enter the ignition regime in this case. When spin polarization of deuterium and ^{3}He ions is introduced [γ_{spin}(D-^{3}He) = 1.5], the ignition boundary becomes wider, and the operation path for $\tau_E = \gamma_H C_{op}/(\bar{P}_{ht} + \bar{P}_F - \bar{P}_b - \bar{P}_s)^{0.5}$ can reach ignition. The D-D fusion suppression effects are not taken into account in this case.

One example is shown in Fig. 5 for checking the ignition access condition in D-^{3}He fusion. The operation path with a height $(\gamma_H C_{op})^2 = 30$ MW/m$^3\cdot$s^2 is just touching the ignition boundary (point A) for $n\tau_E$ two times larger than the saddle point for $\langle\beta\rangle = 6.52\%$, $[\bar{P}_{ht}\tau_E^2]_{SDL} = 7.50$ MW/m$^3\cdot$s^2. (Other parameters are the same as listed above.) We see that the relationship $(\gamma_H C_{op})^2 = 4[\bar{P}_{ht}\tau_E^2]_{SDL}$ is confirmed as expressed in Eq. (5).

IV.B. D-^{3}He Spin Polarization Effect on the Height of the Generalized Saddle Point

The dependence of the height of the generalized saddle point on the degree of the spin polarization

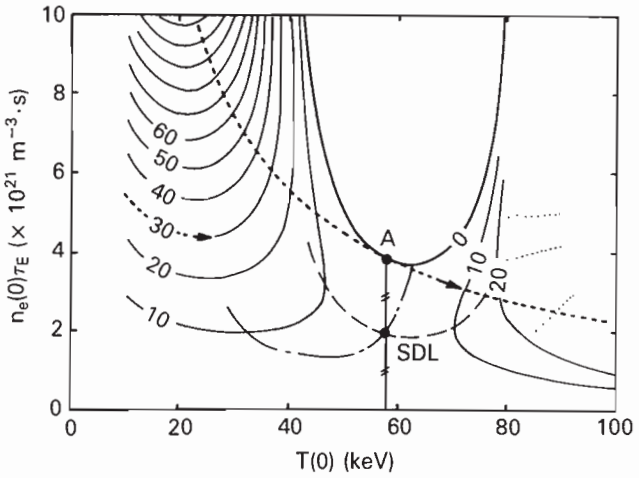

Fig. 5. Operation path with $(\gamma_H C_{op})^2 = 30$ MW/m^3·s^2 for the ACTR-U in the case of complete spin polarization [γ_{spin}(D-^{3}He) = 1.5] and $\langle\beta\rangle = 6.52\%$. Other parameters are the same as in Fig. 4. The height of the saddle point is $[\bar{P}_{ht}\tau_E^2]_{SDL} = 7.50$ MW/m^3·s^2.

γ_{spin}(D-^{3}He) is shown for $\langle\beta\rangle = 5\%$ in Fig. 6a and $\langle\beta\rangle = 10\%$ in Fig. 6b with various profile parameters $\alpha_n = \alpha_T$ using the same parameters as in Sec. IV.A, except for the $\langle\beta\rangle$ values. With complete spin polarization, the height of the generalized saddle point becomes drastically lower, especially in the low-beta regime with broader density and temperature profiles, as shown in Fig. 6a. In the higher beta regime with peaked density and temperature profiles, spin polarization effects are relatively reduced, as shown in Fig. 6b. For example, the height of the generalized saddle point decreases to about one-third for $\langle\beta\rangle = 10\%$ and $\alpha_n = \alpha_T = 1$ with complete spin polarization. If depolarization takes place, the degree of spin polarization has an intermediate value between 1 and 1.5 as in the D-T case, and the height of the generalized saddle point also takes an intermediate value.

Figure 7 shows the dependencies of the height of the generalized saddle point on the $\langle\beta\rangle$ value for three profile parameters with unpolarization and spin polarization, respectively, in the case of $f_D = f_{^3He} = \frac{1}{3}$ and $Z_{eff} = \frac{5}{3}$. The solid curves are for the ACTR-U tokamak with $a = 2$ m; the dashed curves are for ACTR-U with $a = 2.645$ m and a larger plasma current. The dash-dotted lines are for DHETR with a smaller major radius and a crescent plasma shape, with parameters as listed in Table I. The curves for the height of the generalized saddle points for these three tokamaks are similar while the machine size is different. This means that the synchrotron radiation loss is not very different in these machines as long as the wall reflectivity and the hole fraction are the same. Note that the curves for the height of the generalized saddle points for Apollo,[8] listed in Table I, lie between the upper and

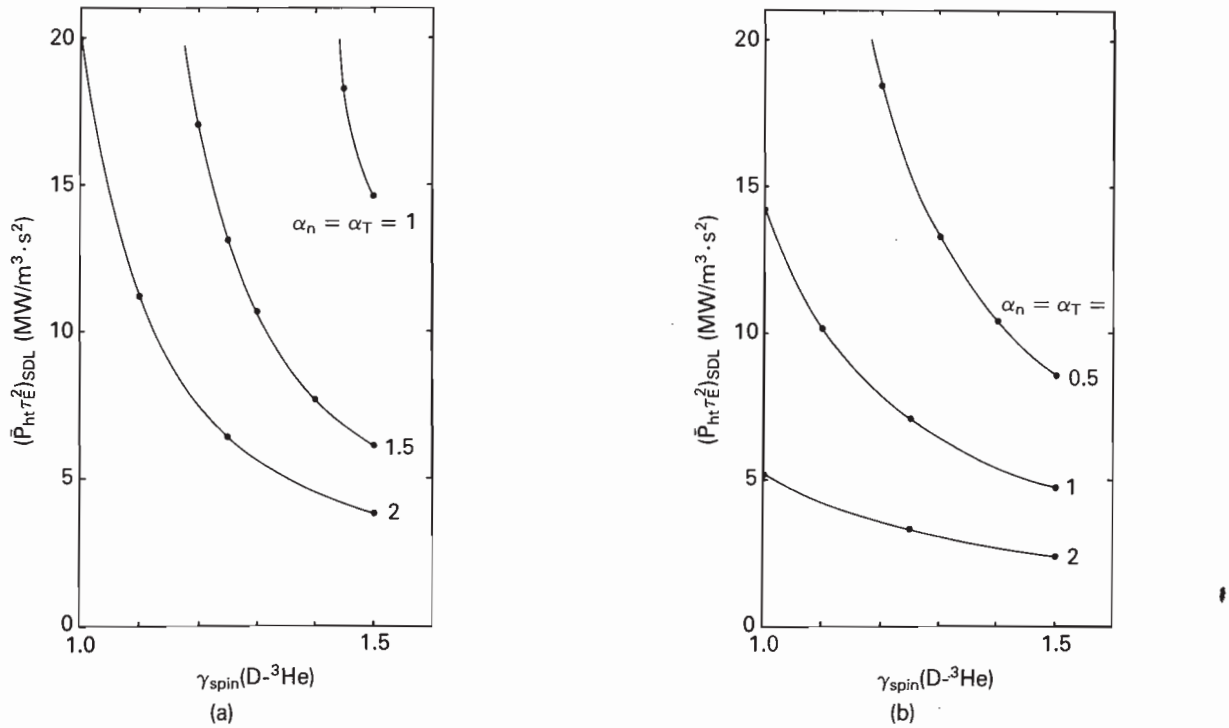

Fig. 6. Height of the generalized saddle point versus spin polarization factor γ_{spin}(D-^{3}He) for various profile parameters $\alpha_T = \alpha_n$ in the case of $\langle\beta\rangle$ = (a) 5% and (b) 10%. Other parameters are the same as in Fig. 4.

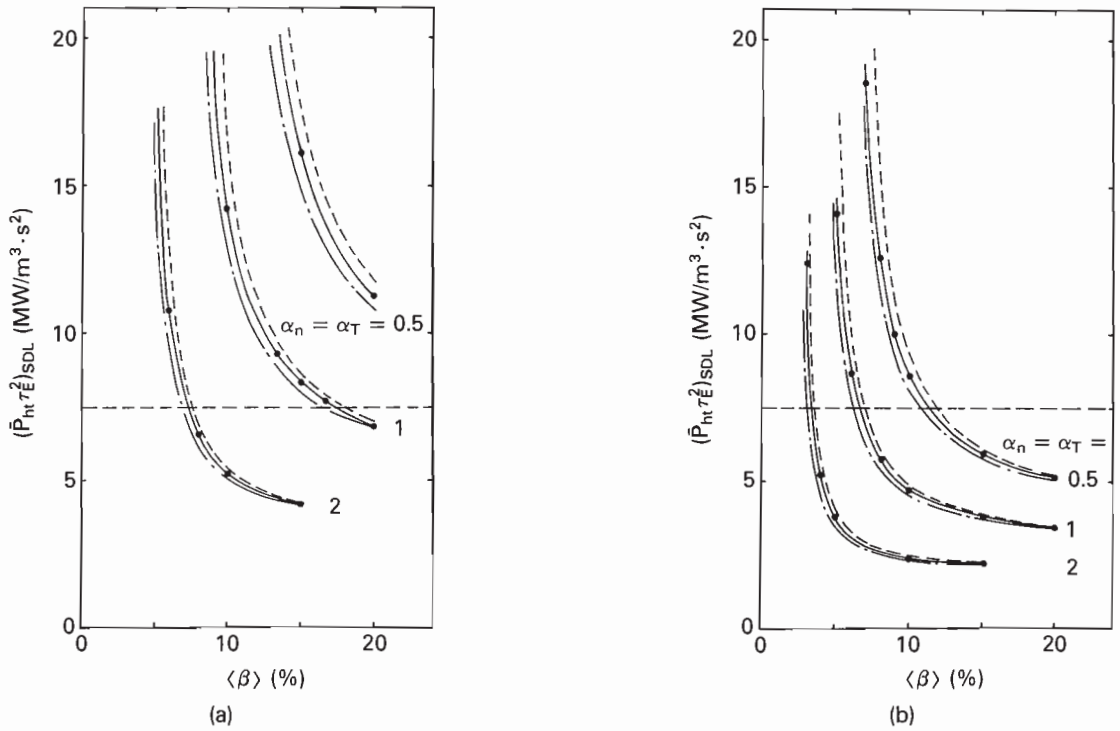

Fig. 7. Height of the generalized saddle point versus the toroidal beta value for various profile parameters $\alpha_T = \alpha_n$ in the case of (a) no spin polarization [γ_{spin}(D-^{3}He) = 1] and (b) complete spin polarization [γ_{spin}(D-^{3}He) = 1.5] for $f_D = f_{^3He} = \frac{1}{3}$. The horizontal dashed line corresponds to the height of the operation path, $(\gamma_H C_{op})^2/4$, where $(\gamma_H C_{op})^2 = 30$ MW/m^3·s^2.

lower curves. The horizontal dashed line corresponds to the height of the operation path divided by 4, that is, $(\gamma_H C_{op})^2/4 = 30/4 = 7.5$ MW/m^3·s^2. The regime satisfying $(\gamma_N C_{op})^2/4 > [\bar{P}_{ht}\tau_E^2]_{SDL}$ is ignition accessible. Thus, this intersection point gives the critical beta value $\langle\beta\rangle_{ig}$ required for ignition in a reactor with the scaling law $\tau_E = \gamma_H C_{op}/(\bar{P}_{ht} + \bar{P}_F - \bar{P}_b - \bar{P}_s)^{0.5}$. Ignition beta values $\langle\beta\rangle_{ig}$ for these tokamaks having the same operation height but different size lie within the range of ±0.8% around the ignition beta value for ACTR-U (solid line). For example, in the case of ACTR-U with $a = 2$ m, $\alpha_n = \alpha_T = 1$, and $(\gamma_H C_{op})^2 = 30$ MW/m^3·s^2, the $\langle\beta\rangle_{ig}$ value is 17% for γ_{spin}(D-^{3}He) = 1, as in Fig. 7a, and 6.5% for γ_{spin}(D-^{3}He) = 1.5 as in Fig. 7b. We also find from this figure that the ignition beta value $\langle\beta\rangle_{ig}$ can be lowered by the choice of a higher operation path. For the broader profile $\alpha_n = \alpha_T = 0.5$, it is impossible to reach ignition within $\langle\beta\rangle = 20\%$ with unpolarization; however, ignition is now accessible at $\langle\beta\rangle_{ig} = 11.4\%$ with spin polarization, as seen from Fig. 7b. We have thus found that spin polarization of deuterium and ^{3}He ions can reduce the ignition beta value drastically and make ignition accessible even for broader density and temperature profiles.

In the case of an optimized fuel mixture ($f_D = 2f_{^3He} = \frac{1}{2}$, hence $Z_{eff} = 1.5$), the height of the generalized saddle point and hence the ignition beta value is further reduced, as shown in Fig. 8a with unpolarization [γ_{spin}(D-^{3}He) = 1] and Fig. 8b with polarization [γ_{spin}(D-^{3}He) = 1.5]. The $\langle\beta\rangle_{ig}$ value at the ignition boundary is 12% for unpolarization in ACTR-U ($a = 2$ m) with $(\gamma_H C_{op})^2 = 30$ MW/m^3·s^2 and $\alpha_n = \alpha_T = 1$. With spin polarization [γ_{spin}(D-^{3}He) = 1.5], $\langle\beta\rangle_{ig}$ is further reduced to 5.3% for the same parameters.

The ignition beta values $\langle\beta\rangle_{ig}$ thus obtained for D-^{3}He tokamaks are summarized in Table III, while the Troyon beta limits calculated by $\langle\beta\rangle_{TROY}$ (%) = 3.5 I_p (MA)/[a (m) B_t (T)] are presented in Table I. When the $\langle\beta\rangle_{TROY}$ value is larger than $\langle\beta\rangle_{ig}$, ignition exists in the first stability regime. Conversely, when $\langle\beta\rangle_{TROY}$ is smaller than $\langle\beta\rangle_{ig}$, ignition needs the second stability regime. By comparing the $\langle\beta\rangle_{ig}$ values in Table I and III, we have found that only the DHETR tokamak could be operated in the first stability regime for unpolarization and spin polarization. Since the DHETR tokamak could be operated in a higher beta regime (up to ~20%) using a highly shaped plasma, the operation regime could be widened. The ACTR-U tokamak with $a = 2$ m needs the second stability regime in both cases, and the ACTR-U tokamak with $a = 2.645$ m and both Apollos can be operated in the first stability regime only when D-^{3}He spin polarization is working. Note that hot-ion mode operation can further reduce the ignition beta value. Also note that fuel

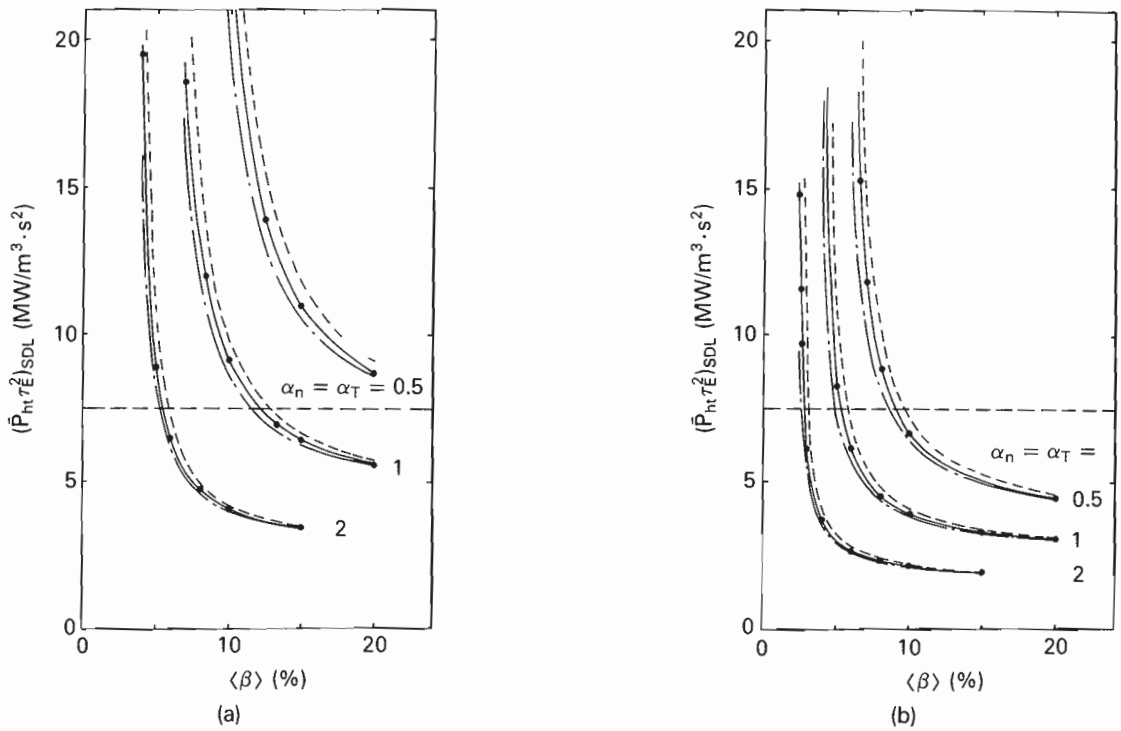

Fig. 8. Same as Fig. 7 except $f_D = 2f_{^3He} = \frac{1}{2}$.

dilution effects due to the impurity content are not taken into account; hence, this calculation is for an ideal case.

IV.C. Confinement Enhancement Factor for Reaching D-^{3}He Ignition

Here, we have adopted as a reference the height of the operation path $(\gamma_H C_{op})^2 = 30$ MW/m$^3\cdot$s^2. To obtain this height, the confinement enhancement factor for a D-^{3}He tokamak reactor should be much larger than 1 (H mode) for the given machine parameters.

From Table I, we can estimate the confinement enhancement factors required to reach ignition. For ACTR-U with $a = 2$ m, $\gamma_H = (30/2.87)^{0.5} = 3.23$ is needed for Goldston scaling and $\gamma_H = (30/1.99)^{0.5} = 3.88$ for the ITER89 power law at $\bar{n} = 5 \times 10^{20}$ m^{-3}. For ACTR-U with $a = 2.645$ m, $\gamma_H = 2.72$ is needed for Goldston scaling and $\gamma_H = 2.93$ for the ITER89 power law at $\bar{n} = 5 \times 10^{20}$ m^{-3}. In the case of DHETR with a crescent plasma shape and 80-MA plasma current, a confinement enhancement factor of 1.78 is required to reach $(\gamma_H C_{op})^2 = 30$ MW/m$^3\cdot$s^2 for Goldston scaling and 1.93 for the ITER89 power law. If a confinement enhancement factor of 2 is obtained as in recent tokamak experiments, the height of the operation path becomes 38 MW/m$^3\cdot$s^2, which corresponds to the horizontal line of $38/4 = 9.52$ MW/m$^3\cdot$s^2 in Fig. 8a; then, the ignition beta value $\langle\beta\rangle_{ig}$ is further reduced from 12.8 to 10.2% for $\alpha_n = \alpha_T = 1$ and $f_D = 2f_{^3He} = \frac{1}{2}$ with unpolarization. For Apollo, with major radii $R = 6$ and 8 m, the confinement enhancement factors $(30/5.98)^{0.5} = 2.24$ and $(30/6.78)^{0.5} = 2.10$, respectively, are necessary to gain a height of operation path $(\gamma_H C_{op})^2 = 30$ MW/m$^3\cdot$s^2 for Goldston scaling. For comparison, the confinement enhancement factor obtained in recent tokamak experiments is 2 to 3.

IV.D. D-D Fusion Suppression Effect by Spin Polarization on Ignition Access Condition

Although D-D fusion suppression due to parallel spin polarization is still controversial and no conclusion has yet been drawn,[11-14] we study here the suppression effect on the ignition access condition for γ_{spin}(D-^{3}He) = 1 and 1.5.

Fueling of spin-polarized ^{3}He by ice pellet would be very difficult because ^{3}He cannot be frozen. However, since fueling of spin-polarized pure deuterium frozen pellets may be possible,[27,28] the D-D fusion suppression effect is important because it can decrease neutron production.

The heights of the generalized saddle points for D-^{3}He unpolarization γ_{spin}(D-^{3}He) = 1 in ACTR-U with $a = 2$ m are shown in Fig. 9a with the complete suppression effect [γ_{spin}(D-D) = 0] (dashed curve) and without the suppression effect [γ_{spin}(D-D) = 1] (solid curve) in the cases of two fuel compositions. The ignition beta value $\langle\beta\rangle_{ig}$ for the height of the operation path $(\gamma_H C_{op})^2 = 30$ MW/m$^3\cdot$s^2 increases from

TABLE III

Minimum Auxiliary Heating Power and Ignition Beta Values in D-^{3}He Tokamak Reactors Evaluated by POPCON and the Ignition Access Condition for Unpolarization and Spin Polarization*

Reactor	V (m^3)	D:^{3}He = 1:1		D:^{3}He = 2:1	
		γ_{spin} (D-^{3}He)			
		1	1.5	1	1.5
		$[\bar{P}_{ht}]_{min}$ (MW/m^3) P_{HT} (MW) $\langle\beta\rangle_{ig}$ (%)		$[\bar{P}_{ht}]_{min}$ (MW/m^3) P_{HT} (MW) $\langle\beta\rangle_{ig}$ (%)	
ACTR-U $a = 2$ m	1579 m^3	0.57 900 17	0.19 MW/m^3 300 MW 6.5%	0.35 550 12	0.14 MW/m^3 220 MW 5.3%
$a = 2.645$ m	2762			0.32 880 11.5	0.125 MW/m^3 345 MW 4.8%
DHETR	995			0.35 350 10.2	0.19 MW/m^3 190 MW 5.3%
Apollo $R = 6.1$ m	1551			0.303 470 12.7	0.148 MW/m^3 230 MW 5.7%
$R = 8$ m	1403			0.96 1347 11.5	0.33 MW/m^3 463 MW 5.1%

*Heights of the operation path are $(\gamma_H C_{op})^2 = 30$ MW/m$^3\cdot$s^2 except for the DHETR tokamak with 38 MW/m$^3\cdot$s^2. Deuterium-deuterium fusion is not suppressed.

12 to 14% for $f_D = 2f_{^3He} = \frac{1}{2}$ and from 17.0 to 18.6% for $f_D = f_{^3He} = \frac{1}{3}$; hence, the D-D spin suppression effect on the ignition access condition is not large. This is because the contribution of D-D fusion power to the total fusion power is relatively small.

In the case of complete spin polarization [γ_{spin}(D-^{3}He) = 1.5] as shown in Fig. 9b, the increase in the height of the generalized saddle point due to D-D fusion suppression is smaller than for γ_{spin}(D-^{3}He) = 1. The value of $\langle\beta\rangle_{ig}$ for the same height of the operation path increases from 5.3 to 5.7% for $f_D = 2f_{^3He} = \frac{1}{2}$ and from 6.5 to 6.7% for $f_D = f_{^3He} = \frac{1}{3}$ with complete D-D fusion suppression [γ_{spin}(D-D) = 0].

IV.E. POPCON Analysis for a D-^{3}He Tokamak

Even if the confinement enhancement factor is sufficient to satisfy the ignition access condition, it is uncertain whether the actual auxiliary heating power to surmount the Cordey pass is acceptable or not. This can be evaluated by a POPCON analysis, not by the ignition access condition.

Figure 10 shows the POPCON plots [$n(0), T(0)$] for ACTR-U ($a = 2$ m) with $\alpha_n = \alpha_T = 1$, $f_D = f_{^3He} = \frac{1}{3}$, and $(\gamma_H C_{op})^2 = 30$ MW/m$^3\cdot$s^2 in the cases of unpolarization and spin polarization, respectively. Constant $\langle\beta\rangle$ lines are drawn by dashed lines, and contour lines of heating power density in units of 0.1 MW/m^3 are shown by solid lines. With unpolarization, ignition exists in the regime of higher central electron density [$n_e(0) > 9.5 \times 10^{20}$ m^{-3}], ion temperature $T(0)$ ~90 keV, and high beta ($\langle\beta\rangle > 17\%$). The minimum auxiliary heating power density to reach ignition is $[\bar{P}_{ht}]_{min} \sim 0.57$ MW/m^3 at the Cordey pass. For ACTR-U with $a = 2$ m and a plasma volume of $V \sim 2\pi^2 R a^2 \kappa = 1579$ m^3, the total heating power is 900 MW, which is excessively large. With complete spin polarization of deuterium and ^{3}He ions, [γ_{spin}(D-^{3}He) = 1.5], the ignition regime becomes so wide that the minimum central electron density is 4.8×10^{20} m^{-3} around 70 keV, and the minimum heating power density is reduced to $[\bar{P}_{ht}]_{min} \cong 0.19$ MW/m^3, as shown in Fig. 10b; this gives an acceptable heating power of 300 MW, three times lower than with unpolarization.

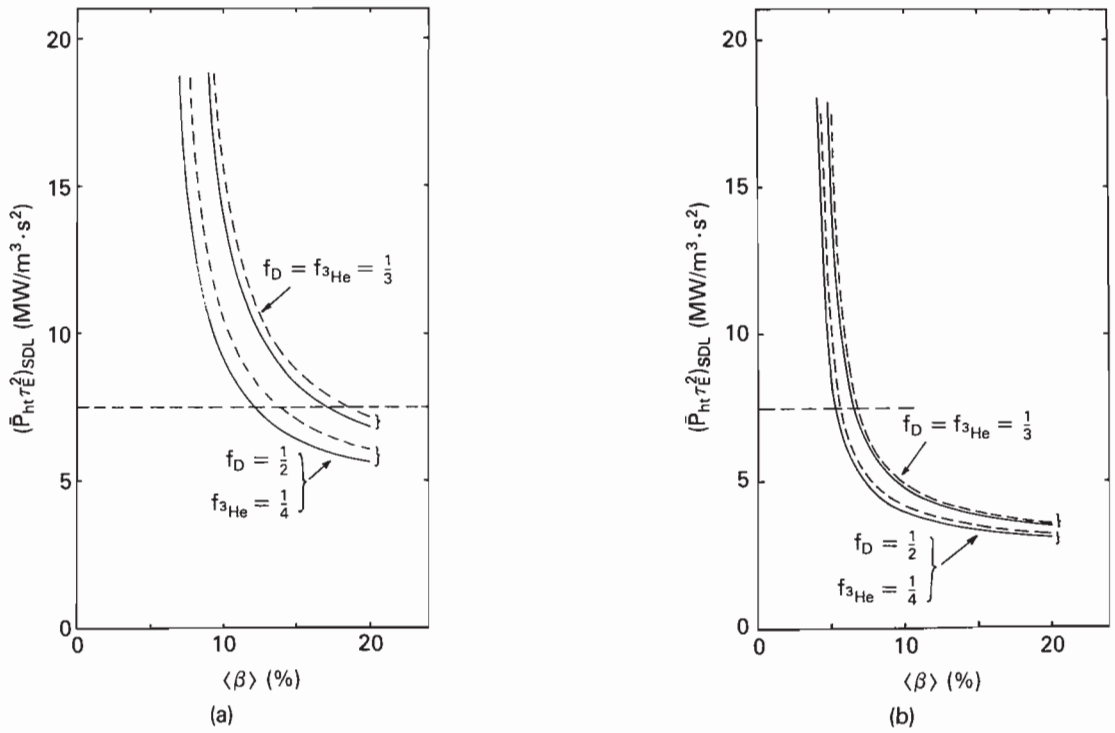

Fig. 9. Dependence of the height of the generalized saddle point on the D-D spin suppression effect for various toroidal beta values in the case of $\alpha_T = \alpha_n = 1$, $f_D = f_{^3He} = \frac{1}{3}$ and $f_D = 2f_{^3He} = \frac{1}{2}$: (a) ^{3}He ions are unpolarized [γ_{spin}(D-^{3}He) = 1] and (b) ^{3}He ions are polarized [γ_{spin}(D-^{3}He) = 1.5]. The dashed lines show the case of complete D-D fusion suppression [γ_{spin}(D-D) = 0], where only D-^{3}He fusion is taking place, and the solid lines indicate no spin polarization of deuterium [γ_{spin}(D-D) = 1].

The minimum toroidal beta value $\langle\beta\rangle_{ig}$ in the ignition regime is 6.52% for complete spin polarization as indicated by point A in Fig. 10b; this corresponds to point A in Fig. 5, where the operation path touches the ignition boundary. We can also confirm that the minimum beta value for ignition obtained from the POPCON analysis is exactly the same as that given by the ignition access condition in Fig. 7b. Note that the two intersection points B and C between the ignition boundary and the $\langle\beta\rangle = 10\%$ constant line in Fig. 10b correspond to points B and C in Fig. 4b.

For the optimum fuel mixture ($f_D = 2f_{^3He} = \frac{1}{2}$), the ignition regime becomes wider even with unpolarization, as shown in Fig. 11a. The minimum heating power density is $[\bar{P}_{ht}]_{min} \sim 0.35$ MW/m^3; hence, the total heating power is ~550 MW for ACTR-U with $a = 2$ m. With spin polarization, the minimum heating power is further reduced to $[\bar{P}_{ht}]_{min} \sim 0.14$ MW/m^3, then 220 MW. With the optimum fuel mixture, the auxiliary heating power can be reduced by a factor of 2.4.

For other D-^{3}He tokamaks, the minimum heating power density $[\bar{P}_{ht}]_{min}$ and total auxiliary heating power P_{HT} are listed in Table III for both unpolarization and spin polarization with D:^{3}He = 1:1 and 2:1 fuel mixtures; the plasma volume $V \sim 2\pi^2 R a^2 \kappa$ is also shown. The ACTR-U ($a = 2.645$ m) and Apollo ($R = 8$ m) tokamaks have excessively large auxiliary heating powers for the unpolarization case. This is due to the large plasma volume in the former tokamak, while the latter has a larger toroidal magnetic field ($B_t = 12.9$ T), which leads to an increase in the synchrotron radiation loss. This indicates that after entering the ignition regime, the toroidal field must be increased to enhance the synchrotron radiation loss for energy conversion, or alternatively, hot-ion mode operation [$T_i(0) > T_e(0)$] must be employed during the heating phase in Apollo with $R = 8$ m. [Note that the auxiliary heating power for Apollo with $R = 8$ m is decreased by a factor of 3 for hot-ion mode operation ($T_i(0)/T_e(0) = 1.2$).] In DHETR and Apollo ($R = 6$ m), the heating power is acceptable with spin polarization. Thus, we have seen that even if the confinement enhancement factor is acceptable, it is uncertain whether the auxiliary heating power to reach ignition is acceptable.

The spin polarization effect is thus found to reduce the auxiliary heating power by one-half to one-third. We should remember that to reach ignition in a certain time interval, the auxiliary heating power must be larger than these minimum values of heating power.

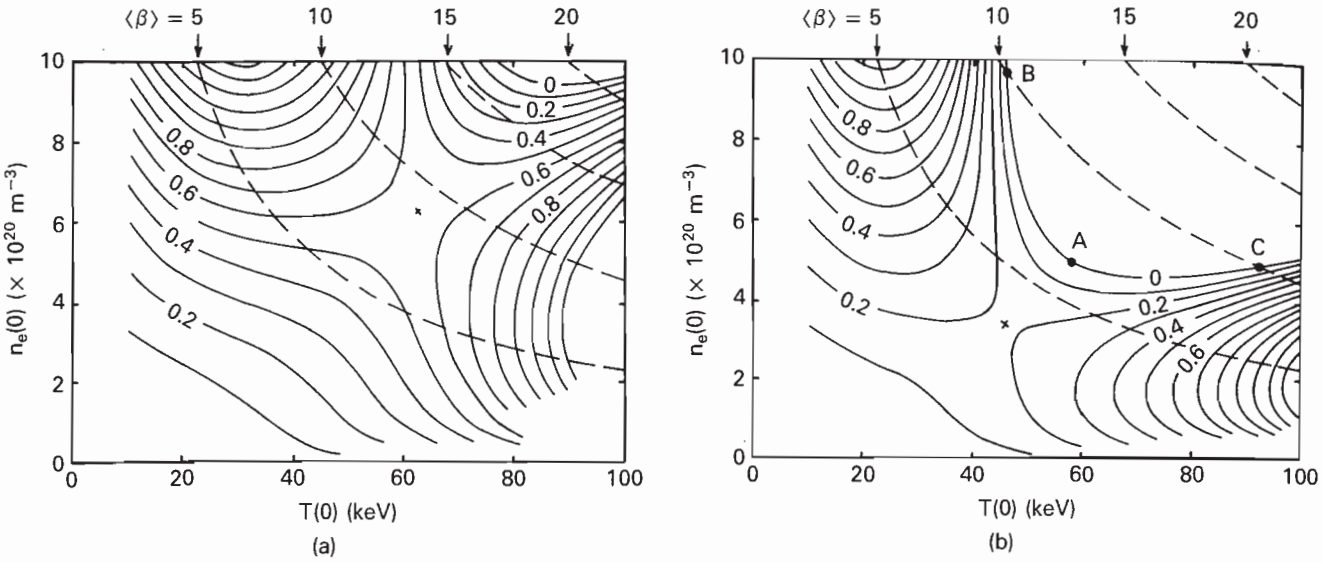

Fig. 10. POPCON analysis [contour lines of constant $\bar{P}_{ht}$ (MW/m^3)] for ACTR-U with (a) no spin polarization [γ_{spin}(D-^{3}He) = 1] and (b) complete spin polarization [γ_{spin}(D-^{3}He) = 1.5] with $f_D = f_{^3He} = \frac{1}{3}$ and $T_i(0) = T_e(0) = T(0)$.

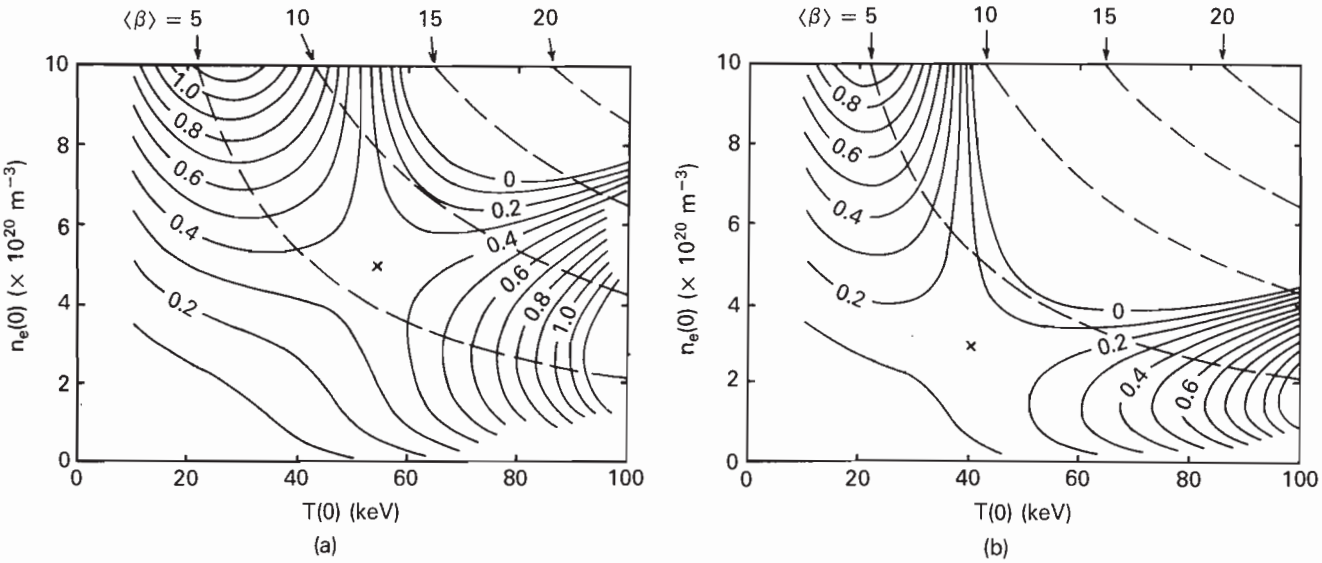

Fig. 11. Same as Fig. 10 except $f_D = 2f_{^3He} = \frac{1}{2}$.

V. DISCUSSION

Recent theory shows that the spin state of fuels cannot be depolarized by ionization or any atomic collision process because the collision time is short and the nuclear spin interaction is very small.[29] However, the nuclear spin polarization state can be destroyed when oscillations or fluctuations of the magnetic field have a left circularly polarized component that resonates with the spin precession frequency.[5,29] Thus, ion cyclotron resonance heating may not be compatible with the use of spin-polarized plasmas because the deuteron cyclotron frequency Ω_D is close to the deuteron precession frequency ($\Omega_{pD} = 0.86\Omega_D$) (Refs. 30 and 31). Perpendicular injection of neutral beams sometimes excites magnetic fluctuations around the ion cyclotron frequency [$\omega \sim n\Omega_D(n = 1,2,3)$] (Ref. 32), which may depolarize the fuel ions.[30,31] Hence, tangentially aligned neutral beam injection may be necessary for spin-polarized plasmas. If a spin-polarized neutral beam can be constructed, it would also serve for fueling. On the other hand, electron cyclotron resonance

heating with $\Omega_e \sim 280$ GHz may be compatible with spin-polarized plasmas. It usually heats the electrons first, giving a hot electron mode with $T_e(0) > T_i(0)$ and leading to a higher generalized saddle point.[7] However, in the high-density D-^{3}He fusion regime, plasmas with $T_i(0) \sim T_e(0)$ could be obtained; then this heating method may be applicable for heating spin-polarized plasmas.

An anisotropic distribution of alpha particles by spin polarization in D-T plasmas induces an instability around the triton spin precession frequency ($\Omega_{pT} \sim 5.96\Omega_D$), which may depolarize tritium nuclei. Instability around the deuteron cyclotron frequency Ω_D may not depolarize deuterons by mode damping if we choose an aspect ratio of <4 (Ref. 33). Note that the aspect ratios of the D-T and D-^{3}He tokamaks listed in Table I are <4 except for the ACTR-U tokamak. In D-^{3}He plasmas, instabilities excited by an anisotropic distribution of 14.7-MeV protons is weak. Therefore, depolarization by this mechanism is not so dangerous[34]; this is a favorable aspect in D-^{3}He spin-polarized plasmas.

The creation of an anisotropic distribution of the fusion products by parallel spin polarization may enhance the loss of fusion products,[24] which leads to smaller η_α, η_{p14}, and so on. If this happens, the total effectiveness of spin polarization can be determined by the product $\eta_\alpha \gamma_{spin}$(D-T) given by Eq. (A.2) in the Appendix for D-T fusion and $\eta_{p14}\gamma_{spin}$(D-^{3}He) together with $\eta_\alpha \gamma_{spin}$(D-^{3}He) given by Eq. (A.6) in D-^{3}He fusion. If these values are >1, or if $\eta_\alpha > 1/1.5$, spin polarization is effective for the ignition condition. This problem could be alleviated by choosing a small toroidal field ripple with a large plasma current.

The most dangerous depolarization might occur at a metallic first wall during recycling.[35] A possible remedy is to use amorphous graphite. However, in a D-^{3}He tokamak reactor, a metallic first wall with a high reflectivity is essential to reduce the synchrotron radiation loss; therefore, dielectric materials such as amorphous graphite may increase the synchrotron radiation loss. Even if the spin polarization state can be maintained by the use of amorphous graphite, the enhanced synchrotron radiation loss may offset the spin polarization effect. Hence, if a metallic first wall can be used for spin-polarized plasmas, it is very attractive for a D-^{3}He reactor. In fact, in some discharges such as "supershots," first-wall recycling is very small for a time when the wall absorbs but does not emit fuels.[30] Recycling takes place only on the limiter or divertor plate. In these cases, if the limiter and divertor are made from amorphous graphite, depolarization may not be a problem. Thus, spin polarization could transiently be used to reduce the auxiliary heating power in the startup phase. The situation is similar in a D-T tokamak reactor with a high toroidal field and a low-beta plasma, where the synchrotron radiation loss becomes large.

For fueling spin-polarized fuel, injection of frozen ice pellets, which can supply a large number of fuel atoms, might be a good method. The low-temperature technique can be combined with microwave radiation to spin flip the iced pellet.[27] Spin polarization of a D-T ice pellet could be produced by dynamic polarization. Tritium decay heat may hinder the cooling of the pellet but may help the dynamic polarization by supplying paramagnetic electrons.[27] A deuterium frozen pellet could also be made in a quite low temperature regime. Recent experiments by Alexander et al.[28] have shown that 38% spin-polarized deuterium ice has been achieved. Fueling of ^{3}He is crucially important in a D-^{3}He fusion reactor. An innovative method for making a ^{3}He pellet overcoated with D_2 ice and a lithium foil shell has been proposed by Wittenberg[36] including polarized ^{3}He fuels; this must be pursued further. Other potentially useful methods of fueling ^{3}He have been discussed by Emmert et al.[37] In the high-temperature D-^{3}He ignition regime, penetration by a D-^{3}He ice pellet would be very difficult. However, if we restrict the use of the pellet only to the startup phase, even though the plasma temperatures there are still higher than in the D-T case, the method would work. The spin-polarized pellet scheme could be useful in the initial phase to help access ignition.

If polarized pellets can be injected into a plasma without any mechanical rotation, the evaporation process is the next major concern. The nuclear spin should not be depolarized by spin/lattice interaction in the heating process and during the evaporation phase of a pellet. We consider depolarization of spin-polarized ions during the diffusive process in the evaporation phase of the pellet. Spin-polarized neutrals are ionized upon evaporation, then expand along the rippled toroidal magnetic field, and experience the perpendicular magnetic field oscillation with a time scale determined by the ripple length L and the expansion speed (comparable with the ion acoustic velocity C_s). In the case of a toroidal coil set with $N_c = 20$, the oscillation frequency of evaporated deuterons is given by $1/t \sim C_s/L = C_s/[2\pi R/N_c] \sim 3 \times 10^5\ s^{-1}$ for $T(0) = 10$ keV and $R = 10$ m, which is two orders of magnitude smaller than the precession frequency ($\Omega_{pD} \sim 0.86\Omega_D = 3.9 \times 10^7\ s^{-1}$ or $\Omega_{pT} \sim 5.96\Omega_D = 2.7 \times 10^8\ s^{-1}$ for $B_t = 6$ T). Thus, we have found that spin depolarization due to toroidal field ripple does not take place during the pellet evaporation phase in a D-T reactor. For D-^{3}He, the situation is similar.

In this study,we have restricted the scaling to relatively pessimistic power law scalings: Goldston and ITER89P. Other types of power law scalings, such as the Kaye-All-Complex[19] and Kaye-Big[38] scalings, were examined in the DHETR tokamak. Since the heights of the operation paths for these scalings are $C_{op}^2 = 4.65$ and $C_{op}^2 = 6.54$ MW/m$^3 \cdot$s^2, respectively, lower than that for the scalings employed in this study, reaching D-^{3}He ignition is more difficult. Note that the offset

linear scaling[22] (ITER89OL) with $\gamma_H = 2$ gives a larger auxiliary heating power than the Goldston scaling but provides a slightly wider D-^{3}He ignition regime because of confinement saturation with high heating power.

We have seen so far that the auxiliary heating power required to reach ignition in D-^{3}He plasmas can be reduced with a D:^{3}He = 2:1 fuel mixing ratio and by aligning the nuclear spin of the deuterium and ^{3}He ions. If hot-ion mode operation [$T_i(0) > T_e(0)$] can be achieved during the heating phase, the auxiliary heating power can be further reduced.[7] For example, the total heating power is decreased by a factor of >3 for $T_i(0)/T_e(0) = 1.5$ in most D-^{3}He tokamaks employed in this study.

If the nuclear elastic scatterings of 14.7-MeV protons[39] are taken into account, hot-ion mode operation can be achieved.[40,41] For example, assuming $T_i(0)/T_e(0) = 1.2$ at $T_i(0) \sim 40$ to 60 keV (Ref. 41) and complete deuterium and ^{3}He spin polarization [γ_{spin}(D-^{3}He) = 1.5], the auxiliary heating power in the DHETR tokamak is reduced to 110 MW from 190 MW [$T_i(0)/T_e(0) = 1$ case].

VI. SUMMARY

Using the generalized ignition contour map and the height of the generalized saddle point, we examined the ignition access condition for unpolarization and spin polarization in a D-T and D-^{3}He tokamak reactor with an isothermal plasma [$T_i(0)/T_e(0) = 1$]. We can summarize the main results as follows.

In a D-T tokamak reactor, spin polarization is very effective when ignition is marginal. The confinement enhancement factor to reach ignition can be lowered by ~20% with complete spin polarization.

In a D-^{3}He tokamak reactor, values of the height of the generalized saddle point of $(\gamma_H C_{op})^2 \approx 30$ MW/m$^3 \cdot$s^2 are necessary to reach ignition for the power law scaling. The confinement enhancement factors to reach this value in the D-^{3}He tokamaks used in this study ranged from 1.78 to 3.23 for Goldston scaling and 1.93 to 3.88 for ITER89 power law scaling with $\bar{n} = 5 \times 10^{20}$ m^{-3}.

The ignition toroidal beta value can be reduced by spin polarization from 12 ± 0.8 to 5.3 ± 0.5% in D-^{3}He = 2:1 plasma and from 17 ± 0.5 to 6.5 ± 0.2% D-^{3}He = 1:1 plasma.

The minimum heating power to reach ignition with complete spin polarization of deuterium and ^{3}He ions can be reduced by a factor of 2 to 3 compared with the unpolarization case. For example, in the DHETR tokamak, 350 MW of auxiliary heating power in a D:^{3}He = 2:1 and $T_i(0)/T_e(0) = 1$ plasma can be reduced to 190 MW with complete polarization. Therefore, operation with spin polarization may be attractive in the startup phase where penetration by D-^{3}He ice pellets could be achieved in the relatively lower temperature, and depolarization on the first wall could be eliminated by low recycling due to wall conditioning before operation.

Deuterium-deuterium fusion suppression due to parallel spin polarization does not affect the ignition condition much, while the neutron flux is reduced by a factor of $1/\gamma_{spin}$(D-D).

Although it is difficult to inject a spin-polarized D-^{3}He ice pellet, the spin polarization scheme is more advantageous in a D-^{3}He fusion reactor than in a D-T fusion reactor.

APPENDIX

The coefficients A_L to A_s in the global power balance equation are given as follows.

D-T Fusion

Detailed derivations have been presented in Refs. 18 and 19. In this case, the synchrotron radiation losses are neglected:

$$A_L = \frac{1.5\{f_D + f_T + 1/[T_i(0)/T_e(0)]\}T_i(0)1.6 \times 10^{-19}}{1 + \alpha_n + \alpha_T} , \tag{A.1}$$

with

$$f_D = n_D/n_e ,$$

$$f_T = n_T/n_e ,$$

$$f_D = f_T = 0.5 - [(Z-2)/(Z-1)]f_\alpha - [(Z_{eff}-1)/(Z-1)]0.5 ;$$

$$A_F = \gamma_{spin}(\text{D-T}) \cdot f_D f_T \cdot (3.52\eta_\alpha) \times \left\{ \int_0^1 (1-x^2)^{2\alpha_n} \langle \sigma v \rangle_{DT} [T_i(x)] 2x\, dx \right\} \times 1.6 \times 10^{-13} , \tag{A.2}$$

where

η_α = alpha-particle heating efficiency

γ_{spin}(D-T) = degree of spin polarization of deuterium and tritium ions

$$A_b = \frac{1.5 \times 10^{-38} Z_{eff} \sqrt{T_e(0)}}{1 + 2\alpha_n + 0.5\alpha_T} \tag{A.3}$$

$$A_s = 0 . \tag{A.4}$$

D-^{3}He Fusion

Detailed derivations have been given in Ref. 7:

$$A_L = \frac{1.5\{f_D + f_{^3He} + 1/[T_i(0)/T_e(0)]\}T_i(0)1.6\times10^{-19}}{1+\alpha_n+\alpha_T} \quad ; \tag{A.5}$$

$$\begin{aligned} A_F = \{&\gamma_{spin}(\text{D-}^3\text{He})\cdot f_D f_{^3He}\cdot(14.7\eta_{p14}+3.7\eta_\alpha)\int_0^1 (1-x^2)^{2\alpha_n}\langle\sigma v\rangle_{\text{D-}^3\text{He}}[T_i(x)]2x\,dx \\ &+\gamma_{spin}(\text{D-D})\cdot f_D^2/2\cdot(3.01\eta_{p3}+1.02\eta_T)\int_0^1 (1-x^2)^{2\alpha_n}\langle\sigma v\rangle_{\text{D-D,T}}[T_i(x)]2x\,dx \\ &+\gamma_{spin}(\text{D-D})\cdot f_D^2/2\cdot(0.82\eta_{^3He})\int_0^1 (1-x^2)^{2\alpha_n}\langle\sigma v\rangle_{\text{D-D,}^3\text{He}}[T_i(x)]2x\,dx\}1.6\times10^{-13} \quad , \end{aligned} \tag{A.6}$$

where the secondary D-T fusion from D-D fusion products is neglected;

$$\begin{aligned} A_b = {}& 1.5\times10^{-38}Z_{eff}\left[\frac{1}{1+2\alpha_n+0.5\alpha_T}+\frac{1}{1+2\alpha_n+1.5\alpha_T}\cdot\frac{2T_e(0)}{mc^2}\right]\sqrt{T_e(0)} \\ &+3\times10^{-38}\left\{\frac{1}{1+2\alpha_n+1.5\alpha_T}+\frac{0.5}{1+2\alpha_n+2.5\alpha_T}\cdot\left[\frac{T_e(0)}{mc^2}\right]\right. \\ &\left.-\frac{3}{1+2\alpha_n+3.5\alpha_T}\cdot\left[\frac{T_e(0)}{mc^2}\right]^2\right\}\frac{2T_e(0)^{1.5}}{mc^2} \quad , \end{aligned} \tag{A.7}$$

where mc^2 is the electron rest energy; and

$$\begin{aligned} A_s = {}& 2.5\times10^{-56}T_e(0)^4\gamma_i^{1.5}\frac{\{f_D+f_{^3He}+1/[T_e(0)/T_i(0)]\}^{1.5}}{\beta(0)^{1.5}(aB_t)^{0.5}}[f_H+(1-f_H)(1-R_{eff})^{0.5}] \\ &\times\int_0^1\left\{(1-x^2)^{0.5\alpha_n+2.5\alpha_T}[1+T_e(0)(1-x^2)^{\alpha_T}/204\,000]\right. \\ &\left.\times[1-\beta(0)(1-x^2)^{\alpha_n+\alpha_T}]^{5/4}\left[\sqrt{T_e(0)}(1-x^2)^{0.5\alpha_T}+\frac{2a}{R}\left(\frac{mc^2}{2\pi}\right)^{0.5}\right]^{0.5}\right\}2x\,dx \quad , \end{aligned} \tag{A.8}$$

with the central toroidal beta value $\beta(0) = \langle\beta\rangle(1+\alpha_n+\alpha_T)$.

ACKNOWLEDGMENTS

One of the authors (O.M.) is grateful to H. M. Skarsgard, University of Saskatchewan, for reading this paper; H. Nakamura, Japan Atomic Energy Research Institute, for sending the information of Ref. 3; and all the faculty members in the Department of Electrical Engineering, Kumamoto Institute of Technology, for encouragement.

REFERENCES

1. S. C. JARDIN, "Physics Overview of CIT," *Proc. 13th Symp. Fusion Engineering*, Knoxville, Tennessee, October 1989, Vol. 2, p. 1265, Institute of Electrical and Electronics Engineers.

2. R. TOSCHI, "The NET Design," *Proc. 5th Int. Conf. Emerging Nuclear Energy Systems*, Karlsruhe, FRG, July 1989, p. 87, Institute of Electrical and Electronics Engineers.

3. E. TADA et al., "The Fusion Experimental Reactor (FER)—Design Concepts," *Proc. 13th Symp. Fusion Engineering*, Knoxville, Tennessee, October 1989, Vol. 1, p. 239, Institute of Electrical and Electronics Engineers.

4. J. R. GILLELAND, Yu. A. SOKOLOV, K. TOMABECHI, and R. TOSCHI, "ITER: Concept Definition," *Nucl. Fusion*, **29**, 1191 (1989).

5. R. M. KULSRUD, H. P. FURTH, E. J. VALEO, and M. GOLDHABER, "Fusion Reactor Plasmas with Polarized Nuclei," *Phys. Rev. Lett.*, **49**, 1248 (1982).

6. L. J. WITTENBERG, J. F. SANTARIUS, and G. L. KULCINSKI, "Lunar Source of ^{3}He for Commercial Fusion Power," *Fusion Technol.*, **10**, 167 (1986).

7. O. MITARAI, A. HIROSE, and H. M. SKARSGARD, "Saddle Point Condition for D-^{3}He Tokamak Fusion Reactor," *Fusion Technol.*, **19**, 234 (1991).

8. G. L. KULCINSKI, G. A. EMMERT, J. P. BLANCHARD, L. A. EL-GUEBALY, H. Y. KHATER, J. F. SANTARIUS, M. E. SAWAN, I. N. SVIATOSLAVSKY, L. J. WITTENBERG, and R. J. WITT, "Apollo—An Advanced Fuel Fusion Power Reactor for the 21st Century," *Fusion Technol.*, **15**, 1233 (1989).

9. B. COPPI and L. E. SUGIYAMA, "Questions in Advanced Fuel Fusion," Laboratory Report PTP-88/6, Massachusetts Institute of Technology (1988).

10. S. ATZENI and B. COPPI, "Ignition Experiments for Neutronless Fusion Reactions," *Comments Plasma Phys. Controlled Fusion*, **6**, 77 (1980).

11. B. P. AD'YASEVICH and D. E. FOMENKO, "Analysis of the Results of the Investigation of the Reaction $D(d,p)/T$ with Polarized Deuterons," *Sov. J. Nucl. Phys.*, **9**, 167 (1969).

12. H. M. HOFMANN and D. FICK, "Fusion of Polarized Deuterons," *Phys. Rev. Lett.*, **52**, 2038 (1984).

13. G. M. HALE and G. D. DOOLEN, "Cross Sections and Reaction Rates for Polarized d + d Reactions," LA-9971-MS, Los Alamos National Laboratory (Feb. 1984).

14. J. S. ZHANG, K. F. LIE, and G. W. SHUY, "Fusion Reactions of Polarized Deuterons," *Phys. Rev. Lett.*, **57**, 1410 (1986).

15. W. A. HOULBERG, S. E. ATTENBERGER, and L. M. HIVELY, "Contour Analysis of Fusion Reactor Plasma Performance," *Nucl. Fusion*, **22**, 935 (1982).

16. N. A. UCKAN and J. SHEFFIELD, "A Simple Procedure for Establishing Ignition Conditions in Tokamaks," *Tokamak Start-Up Problems and Scenarios Related to the Transient Phases of a Thermonuclear Fusion Reactor*, p. 45, H. KNOEPFEL, Ed., Plenum Press, New York (1986).

17. O. MITARAI, A. HIROSE, and H. M. SKARSGARD, "Generalized Ignition Contour Map and Scaling Law Requirement For Reaching Ignition in a Tokamak Fusion Reactor," *Nucl. Fusion*, **28**, 2141 (1988).

18. O. MITARAI, A. HIROSE, and H. M. SKARSGARD, "Generalized Saddle Point Condition for Ignition in a Tokamak Reactor with Temperature and Density Profiles," *Fusion Technol.*, **16**, 197 (1989).

19. O. MITARAI, A. HIROSE, and H. M. SKARSGARD, "Ignition Access Condition Based on the Generalized Saddle Point in a Magnetic Fusion Reactor," Laboratory Report PPL-109, University of Saskatchewan (Feb. 1990); see also *Fusion Technol.*, **20**, 208 (1991).

20. Y. WAKUTA, Y. WATANABE, S. URANO, O. MITARAI, and H. HASUYAMA, "Production of Intense Polarized Atoms and its Application to Tokamak Fusion Reactor," *Proc. 5th Int. Conf. Emerging Nuclear Energy Systems*, Karlsruhe, FRG, July 1989, p. 202.

21. R. J. GOLDSTON, "Energy Confinement Scaling in Tokamaks: Some Implications of Recent Experiments with Ohmic and Strong Auxiliary Heating," *Plasma Phys. Controlled Fusion*, **17**, 87 (1984).

22. P. N. YUSHMANOV, T. TAKIZUKA, K. S. RIEDEL, O. J. W. F. KARDAUN, J. G. CORDEY, S. M. KAYE, and D. E. POST, "Scalings for Tokamak Energy Confinement," *Nucl. Fusion*, **30**, 1999 (1990).

23. O. MITARAI, A. HIROSE, and H. M. SKARSGARD, "Alternating Current Tokamak Reactor with Long Pulses," *Fusion Technol.*, **15**, 204 (1989).

24. E. BITTONI, A. FUBINI, and M. HAEGI, "Enhancement of Alpha Particle Confinement in Tokamaks in the Case of Polarized Deuterium and Tritium Nuclei," *Nucl. Fusion*, **23**, 830 (1983).

25. H. P. FURTH, "Fusion Energy Development: Breakeven and Beyond Keynote Address," PPPL-2500, Princeton Plasma Physics Laboratory (Feb. 1988).

26. H. HASUYAMA and Y. WAKUTA, "Polarized Fusion Reactors," *Genshikaku Kenkyu*, **31**, 35 (1986) (in Japanese).

27. W. HEERINGA, "Prospects for Polarizing Solid DT," *Muon-Catalyzed Fusion and Fusion with Polarized Nuclei*, p. 235, B. BRUNELLI and G. G. LEOTTA, Eds., Plenum Press, New York (1987).

28. N. ALEXANDER, Y. Y. YU, Q. FAN, X. WEI, and A. HONIG, "Metastable (at 4K) Spin-Polarized D in Solid HD as a Polarized Fusion Fuel or Beam Target," *Proc. Annual Mtg. American Physical Society*, Washington, D.C., June 19–22, 1990, paper A6 8, p. 925, American Institute of Physics.

29. R. M. KURLSRUD, E. J. VALEO, and S. C. COWLEY, "Physics of Spin-Polarized Plasmas," *Nucl. Fusion*, **26**, 1443 (1986).

30. P. A. FINN, J. N. BROOKS, D. A. EHST, Y. GOHAR, R. F. MATTAS, and C. C. BAKER, "An Evaluation of Polarized Fuels in a Commercial Deuterium/Tritium Tokamak Reactor," *Fusion Technol.*, **10**, 902 (1986).

31. O. MITARAI, A. HIROSE, and H. M. SKARSGARD, "Reduction of "Ignition Barrier" by Spin Polarized Fusion Reactions," *Genshikaku Kenkyu*, **31**, 59 (1986) (in Japanese).

32. D. K. BHADRA, S. C. CHIU, D. BUCHENAUER, and D. HWANG, "Electromagnetic Emission From a Neutral-Beam-Injected Plasma," *Nucl. Fusion*, **26**, 201 (1986).

33. B. COPPI, S. COWLEY, R. KULSRUD, P. DETRAGIACHE, and F. PEGORARO, "High-Energy Components and Collective Modes in Thermonuclear Plasmas," *Phys. Fluids*, **29**, 4060 (1986).

34. F. PEGORARO, "Depolarization of Spin Polarized Plasmas by Collective Modes," *Muon-Catalyzed Fusion and Fusion with Polarized Nuclei*, p. 179, B. BRUNELLI and G. G. LEOTTA, Eds., Plenum Press, New York (1987).

35. H. S. GREENSIDE, R. V. BUDNY, and D. E. POST, "Depolarization of D-T Plasma by Recycling in Material Walls," *J. Vac. Sci. Technol.*, **A2**, 619 (1984).

36. L. J. WITTENBERG, "Helium-3 Fueling Concepts for Magnetically Confined Fusion," *Proc. 12th Symp. Fusion Engineering*, Monterey, California, Vol. 2, p. 787, Institute of Electrical and Electronics Engineers (1987).

37. G. A. EMMERT, L. El-GUEBALY, G. L. KULCINSKI, J. F. SANTARIUS, J. E. SCHARER, I. N. SVIATOSLAVSKY, P. L. WALSTROM, L. J. WITTENBERG, and R. KLINGELHÖFER, "Possibilities for Breakeven and Ignition of D-^{3}He Fusion Fuel in a Near Term Tokamak," *Nucl. Fusion*, **29**, 1427 (1989).

38. S. M. KAYE, C. W. BARNES, M. G. BELL, J. C. DEBOO, M. GREENWALD, K. RIEDEL, D. SIGMAR, N. UCKAN, and R. WALTS, "Status of Global Energy Confinement Studies," *Phys. Fluids*, **B2**, 2926 (1990).

39. R. W. CONN et al., "Alternate Fusion Fuel Cycle Research," *Proc. 8th Int. Conf. Plasma Physics and Controlled Nucl. Fusion Research*, Brussels, Belgium, July 1980, Vol. 2, p. 621, International Atomic Energy Agency (1981).

40. Y. NAKAO, M. OHTA, and H. NAKASHIMA, "Effect of Nuclear Elastic Scattering on Ignition and Thermal Instability Characteristics of D-D Fusion Reactor Plasmas," *Nucl. Fusion*, **21**, 973 (1981).

41. J. GALAMBOS, J. GILLIGAN, E. GREENSPAN, P. STROUD, and G. H. MILEY, "Discrete Nuclear Elastic Scattering Effects in Cat-D and D-^{3}He Fusion Plasmas," *Nucl. Fusion*, **24**, 739 (1984).